

AD-A158 596

2

OFFICE OF NAVAL RESEARCH

Contract N00014-83-K-142

Task No. NR-631-840

TECHNICAL REPORT NO. 85-1

Acid-Base Behavior of Carboxylic Acid Groups Covalently Attached at the
Surface of Polyethylene: The Usefulness of Contact Angle in Following
the Ionization of Surface Functionality

by

Stephen Randall Holmes-Farley, Robert H. Reamey,
Thomas J. McCarthy, John Deutch, and George M. Whitesides

To be Published in Langmuir

Department of Chemistry
Harvard University
Cambridge, Massachusetts 02138

August 1985

DTIC
ELECTE
AUG 29 1985
S D
G

Reproduction in whole or in part is permitted for
any purpose of the United States Government

This document has been approved for public release
and sale: its distribution is unlimited

DTIC FILE COPY

822 01

REPORT DOCUMENTATION PAGE

1a. REPORT SECURITY CLASSIFICATION Unclassified		1b. RESTRICTIVE MARKINGS	
2a. SECURITY CLASSIFICATION AUTHORITY		3. DISTRIBUTION/AVAILABILITY OF REPORT Approved for Public release. Distribution unlimited.	
2b. DECLASSIFICATION/DOWNGRADING SCHEDULE		4. PERFORMING ORGANIZATION REPORT NUMBER(S) 1	
4. PERFORMING ORGANIZATION REPORT NUMBER(S) 1		5. MONITORING ORGANIZATION REPORT NUMBER(S)	
6a. NAME OF PERFORMING ORGANIZATION Harvard University	5b. OFFICE SYMBOL (If applicable)	7a. NAME OF MONITORING ORGANIZATION ONR	
6c. ADDRESS (City, State and ZIP Code) Department of Chemistry Harvard University Cambridge, MA 02138		7b. ADDRESS (City, State and ZIP Code) Department of Navy Arlington, Virginia 22217	
8a. NAME OF FUNDING/SPONSORING ORGANIZATION ONR	8b. OFFICE SYMBOL (If applicable)	9. PROCUREMENT INSTRUMENT IDENTIFICATION NUMBER	
8c. ADDRESS (City, State and ZIP Code) Department of Navy Arlington, Virginia 22217		10. SOURCE OF FUNDING NOS.	
11. TITLE (Include Security Classification) Acid-Base Behavior of Carboxylic Acid Groups Attached...		PROGRAM ELEMENT NO. N00014-83-K-142	TASK NO. NR 631-840
12. PERSONAL AUTHOR(S) S.R. Holmes-Farley, R.H. Reamey, T.J. McCarthy, J. Deutch, and G.M. Whitesides*			
13a. TYPE OF REPORT Preprint	13b. TIME COVERED FROM _____ TO _____	14. DATE OF REPORT (Yr., Mo., Day) August 1985	15. PAGE COUNT 65
16. SUPPLEMENTARY NOTATION To be published in <u>Langmuir</u>			
17. COSATI CODES		18. SUBJECT TERMS (Continue on reverse if necessary and identify by block number)	
FIELD	GROUP	polymers, contact angle, wetting, surface functionalization, polyethylene, acidities, infrared spectroscopy, XPS, ATR-IR, salt effects, ionization	
19. ABSTRACT (Continue on reverse if necessary and identify by block number)			
<p style="text-align: right;">O-substit</p> <p>Oxidation of polyethylene with chromic acid/sulfuric acid generates a material (PE-CO₂H) having a high density of carboxylic acid and ketone functionalities in a thin surface layer on the polymer. This paper determines the extent of ionization of the surface and near-surface carboxylic acid groups of these materials in contact with water as a function of pH using three experimental techniques: measurement of attenuated total reflectance infrared (ATR-IR) spectra, measurement of contact angles, and direct potentiometric titration. On the basis of correlations between results obtained using these three techniques, we propose an equation relating the contact angle of an aqueous solution having a given value of pH and the extent of ionization (α) of those carboxylic acid groups that are directly exposed to the solution. These carboxylic acid groups have broad titration curves, and have CO₂H groups that are less acidic than soluble carboxylic acids. The initial ionization of these carboxylic acid groups occurs when the solution is</p>			
20. DISTRIBUTION/AVAILABILITY OF ABSTRACT UNCLASSIFIED/UNLIMITED <input checked="" type="checkbox"/> SAME AS RPT <input checked="" type="checkbox"/> DTIC USERS <input type="checkbox"/>		21. ABSTRACT SECURITY CLASSIFICATION Unclassified	
22a. NAME OF RESPONSIBLE INDIVIDUAL Kenneth J. Wynne		22b. TELEPHONE NUMBER (Include Area Code) (202) 696-4410	22c. OFFICE SYMBOL NC

26. Abstract (cont'd)

Oxidation

approximately pH = 6. The detailed structures of these oxidized polymer surface layers and the nature of the interactions between the carboxylic acid and carboxylate ions in them are still not completely defined. Salt effects on the extent of ionization α_1 at a particular value of pH are unexpectedly small, and suggest that charge-charge interactions between carboxylate ions may not dominate the titration curves. This work demonstrates the usefulness of contact angle in following chemical changes occurring in organic functional groups on surfaces. Comparisons of wetting behavior of buffered and unbuffered solutions establishes the importance of using experimental protocols for measuring contact angles in which the reactive groups present in the interfacial region do not outnumber the reactive groups present in the small drop of dilute aqueous solution.

Accession For	
NTIS GRA&I	<input checked="" type="checkbox"/>
DTIC TAB	<input type="checkbox"/>
Unannounced	<input type="checkbox"/>
Justification	
By _____	
Distribution/	
Availability Codes	
Dist	Avail and/or Special
A/1	



11

Introduction. In previous work, we and others have established that oxidation of low-density polyethylene film using chromic acid/sulfuric acid introduces a high density of covalently attached carboxylic acid groups into a thin layer on the surface of the polymer.⁵⁻¹⁵ We have used the resulting material (which we call "polyethylene carboxylic acid", PE-CO₂H, to emphasize the dominant contribution of the carboxylic acid groups to its surface properties) as a substrate in studying phenomena in organic surface chemistry. It has both advantages and disadvantages for this purpose. The advantages are four. It is readily prepared. The presence of carboxylic acid groups on the polymer surface permit the hydrophilicity of the surface to be changed by changing pH (and thus interconverting CO₂H and CO₂⁻ moieties) while leaving the morphology of the surface (approximately) constant. The carboxylic acid moieties provide the basis for a number of convenient methods of surface modification. Results obtained with it are relevant to practical problems in polymer surface chemistry. The major disadvantage is that the functionalized "surface" of PE-CO₂H is heterogeneous and structurally, morphologically, and chemically complex. The surface region is rough on both molecular and macroscopic scales of length. Both carboxylic acid and ketone/aldehyde groups are present in the oxidized layer, in addition to unoxidized methylene groups (and, perhaps, small quantities of methyl, olefin, and alcohol moieties). The oxidized layer has finite (but unknown) thickness, and its composition and structure undoubtedly depends both on its origin (especially the crystallinity of the polymer from which it is derived), on its environment (particularly its access to water), and on its history of thermal and mechanical stress.

This paper is the first of several whose purposes are to develop physical organic techniques for studying the properties of polymer surfaces and functionalized organic monolayer films, to define the nature of the functionalized surface layer of PE-CO₂H and of the model monolayer films, and to use PE-CO₂H and these films to study certain surface properties, especially wetting and adhesion. We use the word "surface" in connection with PE-CO₂H as shorthand for the more accurate but cumbersome phrase "oxidatively functionalized interfacial region," recognizing that the word attributes a simplicity to the interfacial region which does not exist. The primary objective of the present work is an investigation of the relation between the wetting of PE-CO₂H by water and the pH of the water. Its secondary objectives are to explore the utility of contact angle measurements in characterizing surfaces containing an ionizable functional group (here, the CO₂H group) and to examine the ionization of this simple surface functionality. In this study we emphasize those molecular aspects of the surface that contribute directly to changes in the contact angle of water on PE-CO₂H with changes in pH. Later papers will deal with the behavior of ionizable groups other than carboxylic acid moieties, with the influence of the thickness and structure of the oxidized surface on this behavior, with matters such as the extent of hydration and swelling of the oxidized surface, and with differences between the reactivities of functional groups in the surface region in direct contact with bulk liquid water and those of functional groups located deeper in the polymer.

Our emphasis on contact angle measurements as a method of characterizing surfaces containing ionizable groups reflects several considerations. First, experimental measurement of contact angle is straightforward (although not highly precise),^{16,17} and is one of the most convenient methods of characterizing solid/liquid interfaces. We believe that physical organic studies based on wetting of surfaces containing ionizable groups can provide a wealth of information at the molecular level concerning solid/liquid interfaces, and that studies of this type are presently underexploited. Second, acid-base reactions are among the best-understood organic reactions, and comparison of the carboxylic acid moieties of PE-CO₂H with other organic carboxylic acids is useful in establishing characteristic differences between surface and solution reactivity. In particular, we expected PE-CO₂H to behave as a polybasic acid. We address the question: How strongly do the carboxylic acid groups interact, and by what mechanisms? Third, studies of wetting are directly relevant to a range of more complex materials properties of surfaces.

The Relationship between the Contact Angle of Water on PE-CO₂H and the Extent of Ionization of Surface Carboxylic Acid Groups. Acidic water (pH \leq 5) has a greater contact angle on PE-CO₂H than alkaline water (pH \geq 11) (Figure 1). Experimental results outlined in the following sections establish that the basis of this difference is a change in the hydrophilicity of the surface

reflecting ionization of surface carboxylic acid groups. As these groups are transformed to surface carboxylate groups by exposure to the basic aqueous solution, the surface becomes more hydrophilic--that is, the free energy of the solid-liquid interface becomes lower--and the contact angle of the aqueous solution in contact with the surface decreases. In this section we propose a model relating the extent of ionization of the carboxylic acid groups to the contact angle. The experimental data that follow test this model. The physical chemistry of wetting and the theoretical rationalization of contact angle measurements is the subject of a large literature.¹⁶⁻²⁸ We will not review this literature here, but we note that most of these treatments do not address surface structure on the molecular scale.

We follow the simplest model in considering interfacial free energies, and assume that they can be analyzed using three parameters representing the interfacial free energies (γ) at the solid-liquid, liquid-vapor, and solid-vapor interfaces (Figure 2A). Most treatments of wetting omit molecular-level information concerning the interface, and assume the surface to be flat or smoothly rolling and homogeneous. The solid/liquid/vapor system is considered to be at thermodynamic equilibrium. The surface of PE-CO₂H is clearly much more complex than this ideal model (Figure 2B). It is neither flat nor homogeneous. The nature of the three-phase boundary is unclear. The influence of surface-active agents and of other solution components such as salts and buffers (present either intentionally or inadvertently) are difficult to analyze. Although liquid-vapor thermodynamic equilibrium is probably rapidly achieved, the liquid-solid and vapor-solid equilibria are more problematic, since the surface region may swell or rearrange on contact with the liquid phase.

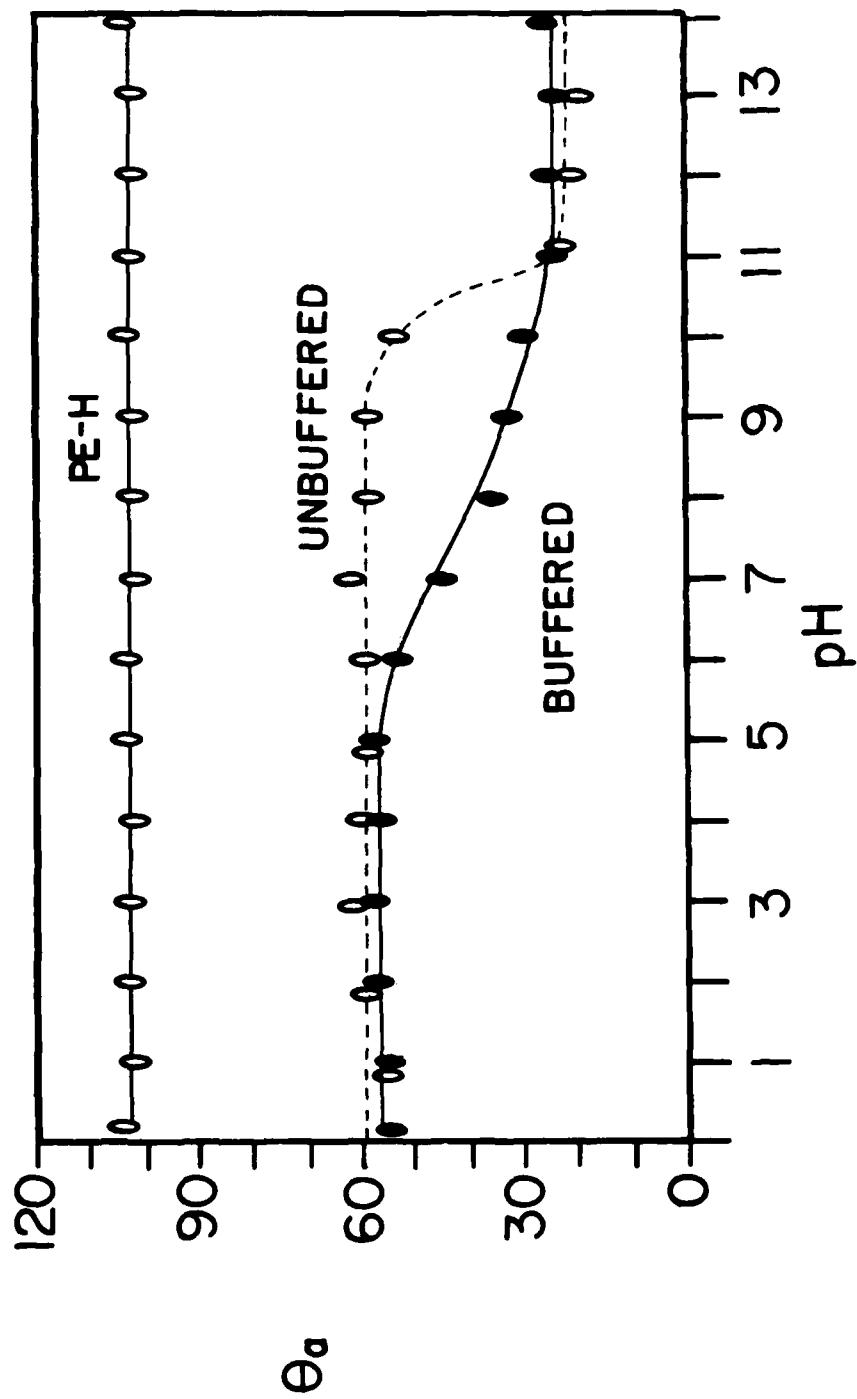


Figure 1. Dependence of advancing contact angle (θ_a) of buffered (●) and unbuffered (○) aqueous solutions on PE-COOH. Unoxidized polyethylene (PE-H) is shown as a control. The buffer used was 0.10 N phosphate.

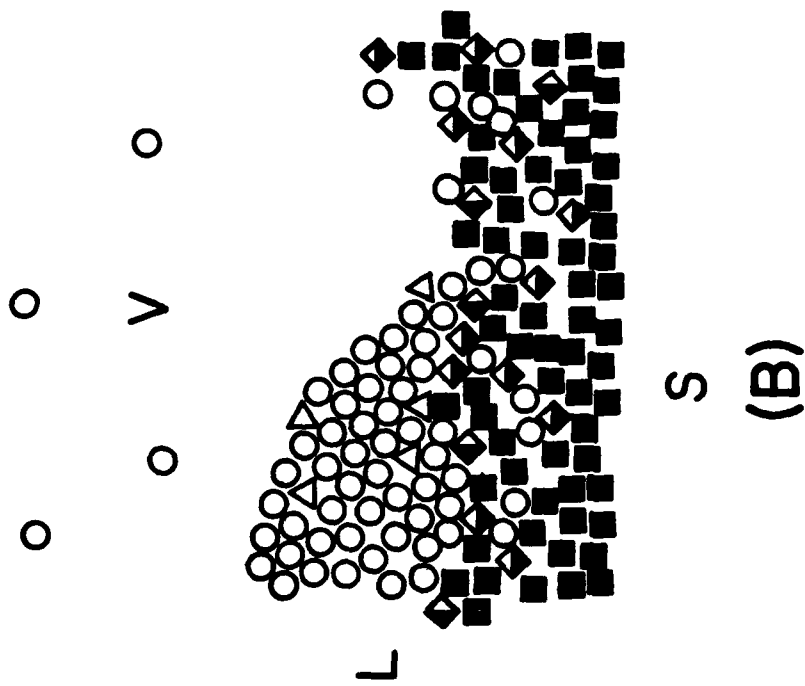
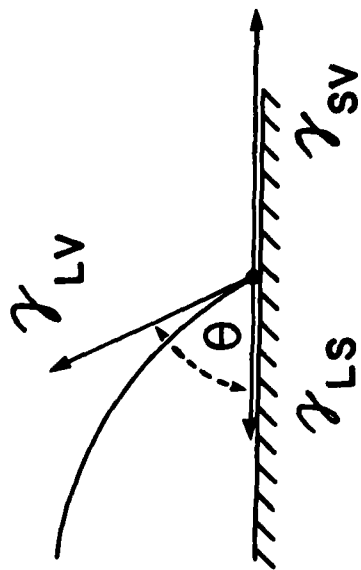


Figure 2. Schematic representations of an ideal (A) and real (B) drop of liquid (L) in contact with solid (S) and vapor (V) with contact angle θ . The symbols in B represent: \circ , water molecules; Δ , dissolved solutes (phosphate, buffer salts; \diamond , \blacklozenge , polar surface groups (CO_2H , CO_2^- , $\text{C}=\text{O}$,...); \blacksquare , nonpolar surface groups (CH_2 , CH_3 ,...)).

Given the complexity of the system of interest at the molecular level, we have proceeded by making three plausible but extreme simplifying assumptions:

i) The surface free energy consists of the sum of contributions from individual groups present at the solid surface and in direct contact with the liquid phase (eq 1).

$$\gamma_{LS} = \sum_j \beta_j \gamma_{LSj} \quad (1)$$

In this equation, β_j is the normalized fraction of a particular type of organic group j in the population of groups in direct contact with the liquid phase ($j = \text{CO}_2\text{H}, \text{CO}_2^-, \text{CH}_2, \text{CH}_3, \text{CHO}, \text{C=O}$, and possibly others for PE-CO₂H) and γ_{LSj} is the value of γ_{LS} for a surface completely covered by the group j ($\beta_j = 1$).

ii) The surface does not reconstruct on changing pH: that is, any change in the extent of swelling with pH does not change the relative population of groups on the surface.

iii) Changes in wetting of the surface with changes in pH are dominated by γ_{LS} : γ_{LV} and γ_{SV} can be considered to be independent of pH.

The first assumption is the equivalent of the assumption that γ_{LS} is determined only by the energy of interaction of the liquid phase with the collection of groups on the exterior surface of the solid; groups in the subsurface region do not influence γ_{LS} . Only groups in direct van der Waals or hydrogen-bonding contact with the overlying water contribute; long-range interactions involving non-adjacent groups are not important. The second assumption is probably unjustified in detail, but is necessary in constructing a tractably simple model. The third assumption can be checked experimentally: the contact angle of water on surfaces containing no

ionizable groups is independent of pH (Figure 1 and further examples below).²⁹ With these assumptions, the only molecular-level changes that should influence γ_{LS} for PE-CO₂H on changing pH are those reflecting ionization of the carboxylic acid moieties (or, in principle, of other groups having value of pK_a between 1 and 13).

We relate the measured contact angle of a small drop of aqueous solution at known pH to the extent of ionization of surface carboxylic acid groups using the following argument. The relation between the important interfacial free energies is given by Young's³⁰ equation (eq 2).¹⁶ With the assumption that the only phenomenon influencing the contact angle of aqueous solutions of

$$\gamma_{LS} + \gamma_{LV} \cos \theta = \gamma_{SV} \quad (2)$$

$$\alpha_i = \frac{[CO_2^-]}{[CO_2^-] + [CO_2H]} \quad (3)$$

$$\alpha_i(pH) = \frac{\gamma_{LS}(pH 1) - \gamma_{LS}(pH)}{\gamma_{LS}(pH 1) - \gamma_{LS}(pH 13)} \quad (4)$$

$$\alpha_i(pH) = \frac{\gamma_{LS}(pH 1) + \gamma_{LV} \cos \theta_{pH} - \gamma_{SV}}{\gamma_{LS}(pH 1) - \gamma_{LS}(pH 13)} \quad (5)$$

$$\alpha_i(pH) = \frac{\cos \theta_{pH} - \cos \theta_{pH 1}}{\cos \theta_{pH 13} - \cos \theta_{pH 1}} \cong \frac{\delta \cos \theta_a(pH)}{\Delta \cos \theta_a} \quad (6)$$

different pH on PE-CO₂H is ionization of the carboxylic acid groups, we can relate the degree of ionization α_i of the surface carboxylic acid groups

(eq 3) to the liquid-solid interfacial free energies at limiting values of pH for which the surface carboxylic acid groups are entirely protonated (pH 1) or completely ionized (pH 13) (eq 4). The assumption underlying eq 4--that the change in the liquid-solid interfacial free energy $\delta\gamma_{LS}$ with changes in pH depends linearly on the fraction of carboxylic acid groups converted to carboxylate ions α_i --is central to the analysis which follows. Representative experimental data (Figure 1) indicate that the contact angle of water on PE-CO₂H is constant and independent of pH between pH 1 and pH 5, and again independent at values of pH greater than 11. We assume the value at pH 1 ($\theta_a = 55^\circ$) to be that characteristic of PE-CO₂H, and the value at pH 13 ($\theta_a = 22^\circ$) to be that characteristic of completely ionized PE-CO₂⁻. With the assumption that γ_{LS} is related linearly to α_i , and that γ_{SV} and γ_{LV} are independent of pH for any given system of buffers, simple manipulation relates α_i to experimental values of the contact angle (eqs 5 and 6; in eq 6, the terms $\Delta \cos \theta_a$ and $\delta \cos \theta_a$ (pH) represent the experimentally relevant differences in contact angles).

Several of the features of this treatment deserve brief comment. First we note that we make no assumption concerning the population of CO₂H (CO₂⁻) groups on the surface of PE-CO₂H (β_{CO_2H} , eq 1). Other evidence indicates that approximately 60% of the oxygen containing functional groups present in PE-CO₂H are CO₂H moieties, and that the remainder are ketone/aldehyde groups.⁵ What fraction of these CO₂H groups is on the exterior surface of PE-CO₂H and influences the contact angle remains to be established. Further it is not yet clear what portion of total groups on the exterior surface of PE-CO₂H is CO₂H groups (rather than ketone, methylene, or other groups), but presently available information suggests a value of $0.2 < \beta_{CO_2H} < 0.5$.³¹ Second, we have assumed that all of the features of the surface, other than

the extent of ionization of the carboxylic acid groups, are independent of pH: that is, in particular, that any changes in surface roughness and extent of swelling or hydration of the surface layer with pH do not influence the contact angle.

A full discussion of experimental evidence relevant to this assumption is beyond the scope of this manuscript, and will be the subject of a separate paper. In brief, however, we note that evidence based on studies of acid-base behavior of PE-CO₂H and on fluorescence spectroscopy of PE-CO₂H having dansyl (dimethylaminonaphthalene sulfonamido) groups covalently bonded to its surface suggests the existence of a thin "gel" layer on this surface, with the majority of the CO₂H groups lying just below the surface.³² This layer does appear to swell in contact with water, and may swell differently at different values of pH. Moreover, this swelling and accompanying proton transfer reactions may extend beyond the edge of drop--that is, that proton transfer equilibria and hydration may occur in the part of the surface layer surrounding the drop which is apparently "dry", without the requirement for an overlying liquid phase. These observations all indicate that the behavior of the surface is complex. In fact, however, despite the potential for intractable complexity, the experimental data summarized in the following sections of this paper suggest that eq 6 provides a useful and reasonably accurate description of the relation between pH, extent of ionization α_j , and contact angle for PE-CO₂H. This agreement between the model and experiment provides a justification for otherwise tenuous approximations.

Contact Angle Measurements: Buffered vs Unbuffered Solutions.

Throughout this work we use two different types of experiments to explore the ionization of surface carboxylic acid groups as a function of pH (Figure 1). One is based on measurement of the contact angle using sessile drop techniques with buffered solutions. The second uses unbuffered solutions. These two

types of experiments generate different curves, and yield different types of information, when applied to the same sample. The difference between them stems from the fact that the density of carboxylic acid groups on the surface of PE-CO₂H is sufficiently high that, for a small drop of dilute unbuffered aqueous base, the system is effectively buffered by the surface CO₂H groups themselves--that is, the number of carboxylic acid groups available for reaction on the polymer surface is larger than the number of hydroxide ions in the drop of water. This argument is best illustrated using a specific example. At pH 8, a 1- μ L drop of water (typical of the size used in this work) contains $\sim 6 \times 10^{11}$ hydroxide ions. If we assume the density of carboxylic acid groups on the surface to be that for a close-packed fatty acid monolayer ($5 \times 10^{14} \text{ cm}^{-2}$),³³ the number of carboxylic acid groups on the surface covered by the drop would be 2×10^{13} (a drop with $\theta = 55^\circ$ covers $\sim 3.4 \text{ mm}^2$). In fact, although the packing of carboxylic acid groups on the exposed surface of PE-CO₂H is probably less than monolayer coverage, the surface is rough and the observed density of CO₂H groups would, as a result, be higher than that for an ideal, planar surface. In addition, the CO₂H groups in the subsurface region, which do not directly influence θ_a , are also accessible to the basic solution and contribute to the buffering capacity of the surface. The measured density of carboxylic acid groups on real, rough PE-CO₂H is approximately four times higher than that for idealized planar monolayer packing.⁵ Hence, the number of carboxylic acid groups involved in proton transfer equilibrium with the aqueous drop for PE-CO₂H is $\sim 7 \times 10^{13}$. The number of carboxylic acid groups at the PE-CO₂H/water interface is therefore larger than the number of hydroxide ions originally present in the drop applied to the surface by a factor of ~ 100 . For small drops and high

surface densities of carboxylic acid groups, the system is buffered by this surface functionality.

The curve of θ_a vs pH obtained using sessile drops of unbuffered solution (Figure 1) is not a titration curve in the usual sense: rather, it represents a type of semi-quantitative counting of carboxylic acid functionalities. The break point in this curve (pH 10, 6×10^{13} hydroxide ions) represents the point in which the buffering due to the CO_2H groups on the polymer surface fails: at this point, the number of hydroxide ions added to the system is approximately equal to the number of carboxylic acid groups and a significant fraction of the carboxylic acid groups exist in the form of carboxylate anions. This break does not represent the pK_a of the surface carboxylic acid groups. Thus, by using constant drop size and increasingly alkaline, unbuffered solutions, it is possible to estimate the number of surface carboxylic acid groups present at the interface. To obtain the pK_a of the surface groups, it is necessary to analyze the curves obtained with buffered drops, and this analysis is one subject of the paper.

The Relation Between the Contact Angle of a Drop and the Surface Area Under It. The illustration in the preceding section indicates that the surface area under a drop is important in estimating the number of surface groups in contact with the drop. For drops with small contact angles, the assumption of a hemispherical shape for the drop leads to serious error. Instead, we consider the drop as part of a larger sphere (Figure 3). In actuality all drops deviate from a spherical contour due to gravitational perturbations, but for the drop size used ($1 \mu\text{L}$) the deviation from spherical is negligible.³⁴ For the dimensions for the drop sketched in Figure 3, simple calculation (summarized in supplemental material in the microfilm edition) yields eq 7 as the relation between S (the idealized planar area under the

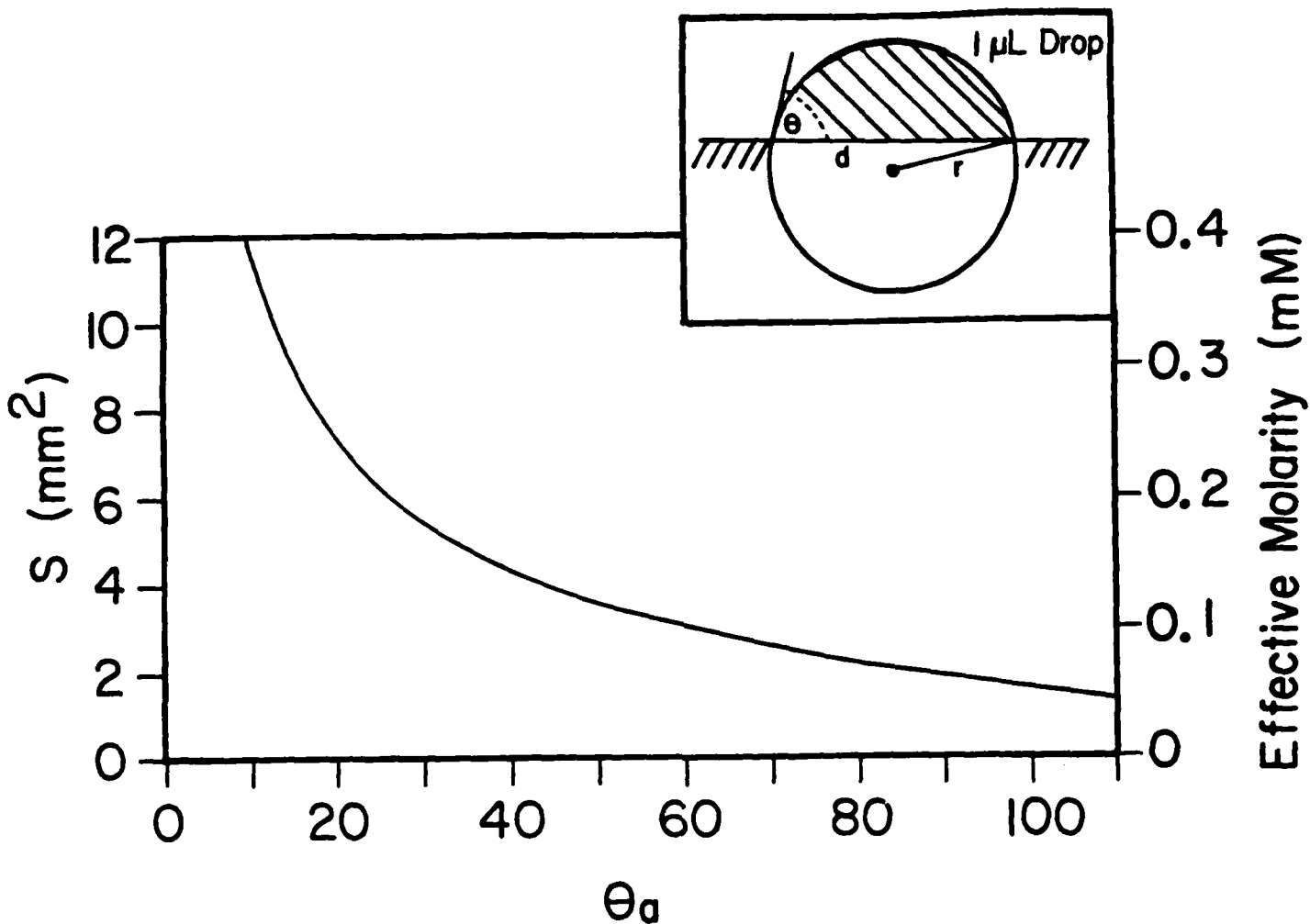


Figure 3. Surface area (idealized planar area, mm²) and effective concentration of surface groups (mM) under a 1- μ L drop, for various values of θ_a , calculated using eq 7. The construction used to arrive at eq 7 is shown at the top of the figure. The shape of the drop is assumed to be a portion of a sphere of radius r . The density of CO₂H groups is assumed to be 20×10^{14} cm⁻² (that is, the measured density on PE-CO₂H; for a planar close-packed monolayer, the values of effective molarity given in the figure should be divided by ~ 4).

drop), V (the volume of the drop) and θ . Figure 3 also summarizes this relationship for the experimental system used in this work: $V = 1 \mu\text{L}$ and a surface density of CO_2H groups of $20 \times 10^{14} \text{ cm}^{-2}$.

$$S = \left[\frac{1}{3} V^{2/3} \sin^2 \theta \right] \left[\frac{2}{3} - \cos \theta + \frac{\cos^3 \theta}{3} \right]^{-2/3} \quad (7)$$

Results and Discussion

Polyethylene. We have examined the surface functionality produced on oxidation of both low-density and ultra high molecular weight polyethylene, although the major part of the research has used the former. All samples were commercial. Low-density polyethylene in the form of film samples from a number of suppliers had similar although not identical characteristics. All of the results reported in this work were obtained using commercial, biaxially oriented, blown low-density film ($\rho = 0.92$) from one supplier, unless otherwise noted. Before oxidation the film was suspended in refluxing methylene chloride for 24 h to remove antioxidants and other film additives. In some instances the film was annealed before extraction by heating at 100°C for several days to relieve some of the stresses introduced in production. Most of the work reported here used unannealed film. Ultra high molecular weight polyethylene was used in the form of rigid sheets, or as high surface area chips generated from this sheet. This material was extracted before use but was not annealed. Low density granular (powder) polyethylene was used without pretreatment.

Oxidation. Polyethylene film and sheet was oxidized by floating appropriately sized pieces on the surface of an $\text{H}_2\text{O}/\text{CrO}_3/\text{H}_2\text{SO}_4$ (42:29:29 w:w:w) solution at 72°C ; UHMW chips and low density grains were oxidized as a

suspension. The advantage of an oxidation procedure for film and sheet involving only one side is that the unoxidized side provides a useful control for later analyses: if, for example, a later reaction changes the contact angle on the control side as well as on the oxidized side, it is probable that non-covalently bound molecules have adsorbed onto the surface of the polyethylene. The oxidized samples of film were rinsed several times with distilled water and acetone, and stored. We reserve the designation PE-CO₂H for oxidized low-density film. Material obtained by oxidation of ultra high molecular weight sheet will be called UHMW-CO₂H, and granular material prepared by oxidation of polyethylene particles as granular PE-CO₂H.

Figure 4 summarizes the influence of the reaction time used for oxidation on the wetting behavior of the polyethylene film and sheet. We draw two conclusions from this plot. First, the contact angle of water on the film reaches a constant value in approximately 60 sec. We believe that the surface composition of the film does not change after the contact angle has reached values of $\theta_a = 55^\circ$ (pH 3) or $\theta_a = 22^\circ$ (pH 12). At the time the films first reach these values of contact angle, their surface morphology is similar to that of unoxidized film by scanning electron microscopy (see below): that is, there is little visible etching of the surface. Prolonged oxidation leads to a much more heavily etched, rougher surface. Nonetheless, the wetting behavior of lightly and heavily oxidized surfaces are indistinguishable. The

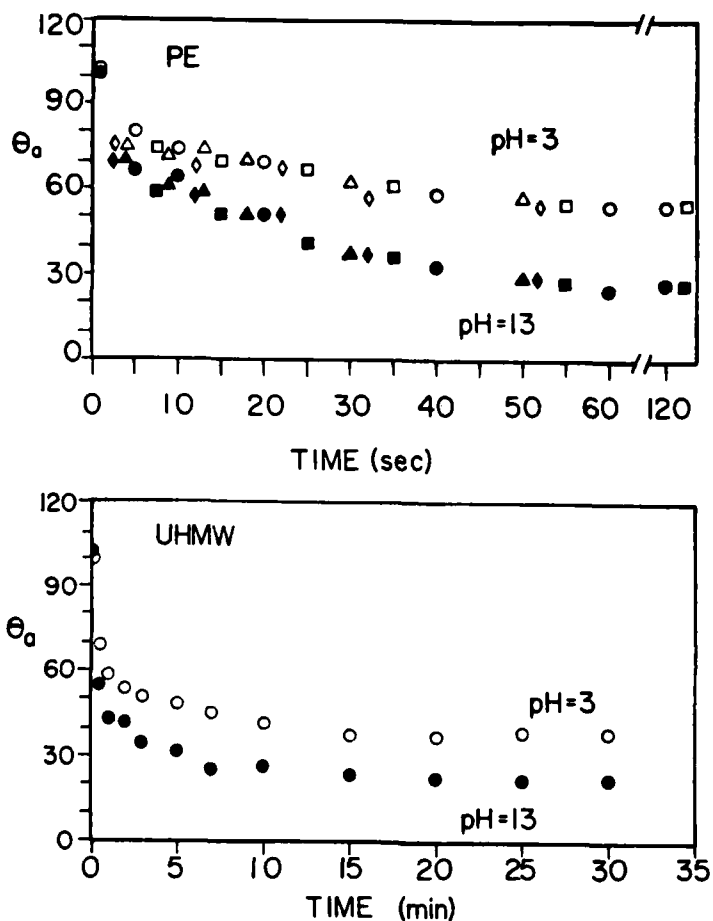


Figure 4. Advancing contact angle for water at pH=3 (HCl, open symbols) and pH=13 (NaOH, filled symbols) for samples of low density polyethylene film (PE) and ultra high molecular weight polyethylene sheet (UHMW) oxidized for times indicated, using the standard procedure (see Text): \circ , \bullet , unannealed; \square , \blacksquare annealed 100 °C for 96 h; \diamond , \blacklozenge annealed 110.6 °C, 24 h; \triangle , \blacktriangle unannealed Monsanto K-2400-212 polyethylene. Extended oxidation of either material increases the roughness of the surface, but does not change the contact angle at pH 3 or pH 13.

use of annealed films has no influence on the course of the oxidation reaction. The changes in wettability of UHMW sheet on oxidation are similar to those for low-density film, although the rate of reaction is slower.

Once prepared, the surface properties of samples of PE-CO₂H are stable on storage at room temperature and gentle manipulation. Figure 5 summarizes values of contact angle as a function of time for storage under different circumstances. If the samples are intentionally exposed to a hydrocarbon-contaminated atmosphere, the surfaces slowly become more hydrophobic. Adsorbed hydrophobic impurities can be removed by washing with diethyl ether. Under a variety of convenient storage conditions, however, the hydrophilicity of the surface remains constant for prolonged periods of time. Infrared and ESCA spectroscopy also reveal no contamination or reconstruction on storage.

The stability of the surface, and its resistance to contamination on storage, are perhaps surprising. Mechanisms for reconstruction--that is, spontaneous thermal migration of surface functionality into the interior of the film--have been studied carefully, and are the subject of a separate paper. It is not clear why these surfaces are more resistant to contamination, as measured by contact angle, ESCA or ATR-IR spectroscopy, than surfaces such as gold.³⁵

The films are handled using tweezers. Mechanical stress of the type experienced by the film in the local area of contact with the tweezers does change wetting characteristics. The modest stresses involved in flexing the film do not, however, seem to do so. Thus, no particular precautions are required to avoid mechanical deformation and stress during routine handling of the sample.

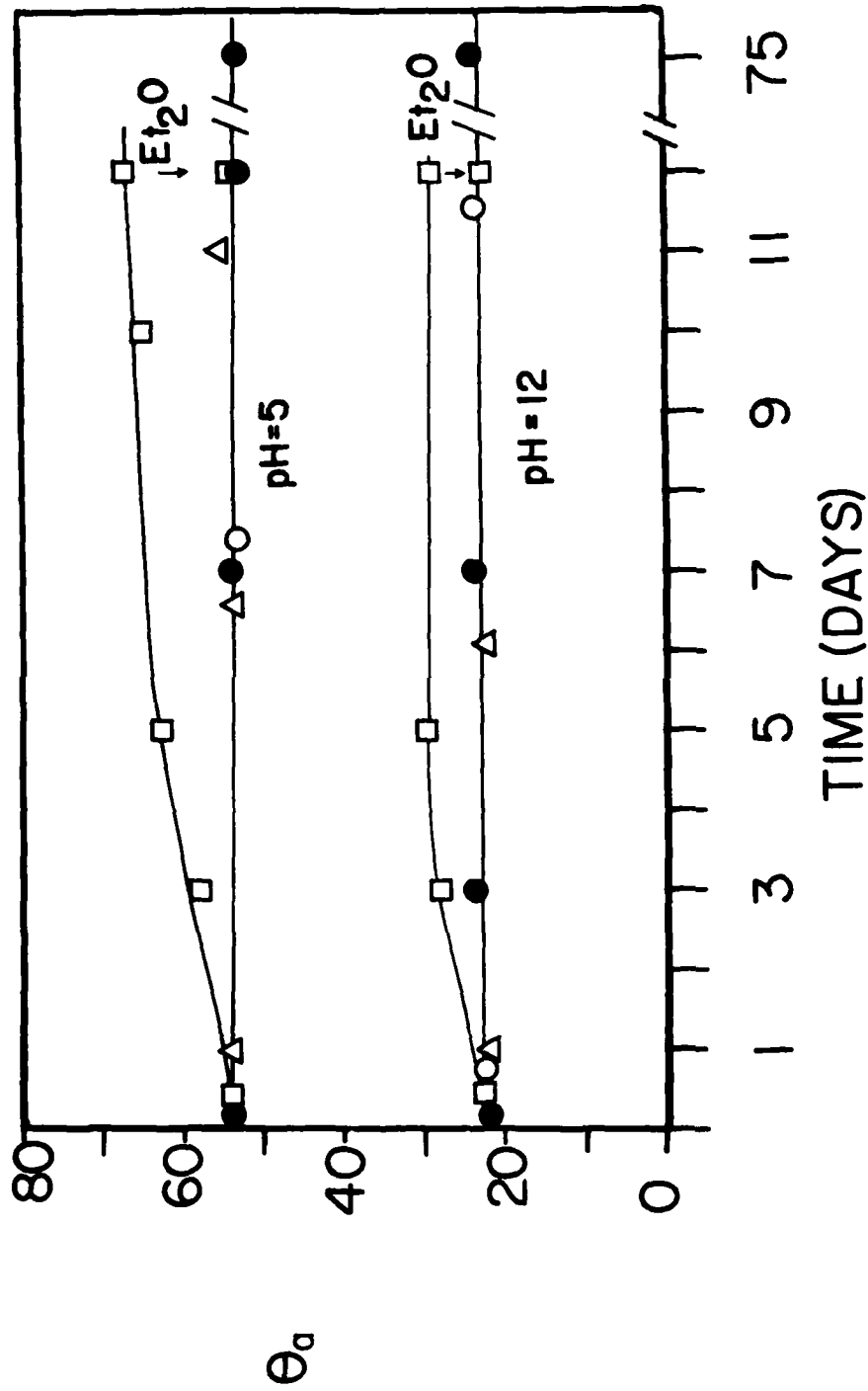


Figure 5. Variation of contact angle (using water at pH 5 and pH 12) of PE-CO₂H with time of storage under different conditions. Films were not previously annealed; T = 20 °C. Storage conditions:

- under dry argon; ○, under argon saturated with water vapor; △, under water; □, exposed to laboratory atmosphere.
- Note that rinsing with ether removed the hydrophobic contaminants adsorbed on the surface of the films.

Characterization of Polymer Surface Functionality

Spectroscopic Techniques. The techniques used to characterize the functionality present on the surface of PE-CO₂H film resemble those described previously, and reach similar conclusions.^{5,6} These will only be outlined here. We have not carried out similarly detailed characterization of the functionality present on the surface of UHMW sheet, but we presume, on the basis of the similarity of its properties to those of low-density film, that acid and ketone/aldehyde groups are also the major functionality of this material. We do not, however, assume that the molecular level structures of the oxidized surfaces are the same. Figure 6 summarizes ATR-IR spectra of samples of polyethylene film in unoxidized form (for reference); following oxidation; following treatment with base (0.1 N NaOH) after oxidation; following reaction with NaBH₄ (a treatment which reduces ketones and aldehydes but leaves carboxylic acids unchanged); and following treatment with diborane (a treatment which reduces both carboxylic acid and ketone groups to alcohol groups). No functionality other than carbonyl functionality is evident in the spectra obtained following oxidation. Treatment of PE-CO₂H with sodium borohydride lowers the intensity of the carbonyl absorption by ~20%. Treatment of the borohydride-reduced sample with aqueous base shifts the absorption at 1710 cm⁻¹ to 1560 cm⁻¹ (carboxylate anion); essentially no absorption remains at 1710 cm⁻¹. These data suggest that both ketones and/or aldehydes and carboxylic acid groups are present in PE-CO₂H. Comparison of the absorption intensities for these samples indicates that the ratio of carboxylic acid to ketone functionalities on the surface is approximately 60:40.³⁶ Despite the fact that ketonic groups represent a significant fraction of the surface functionality, we continue to refer to this material

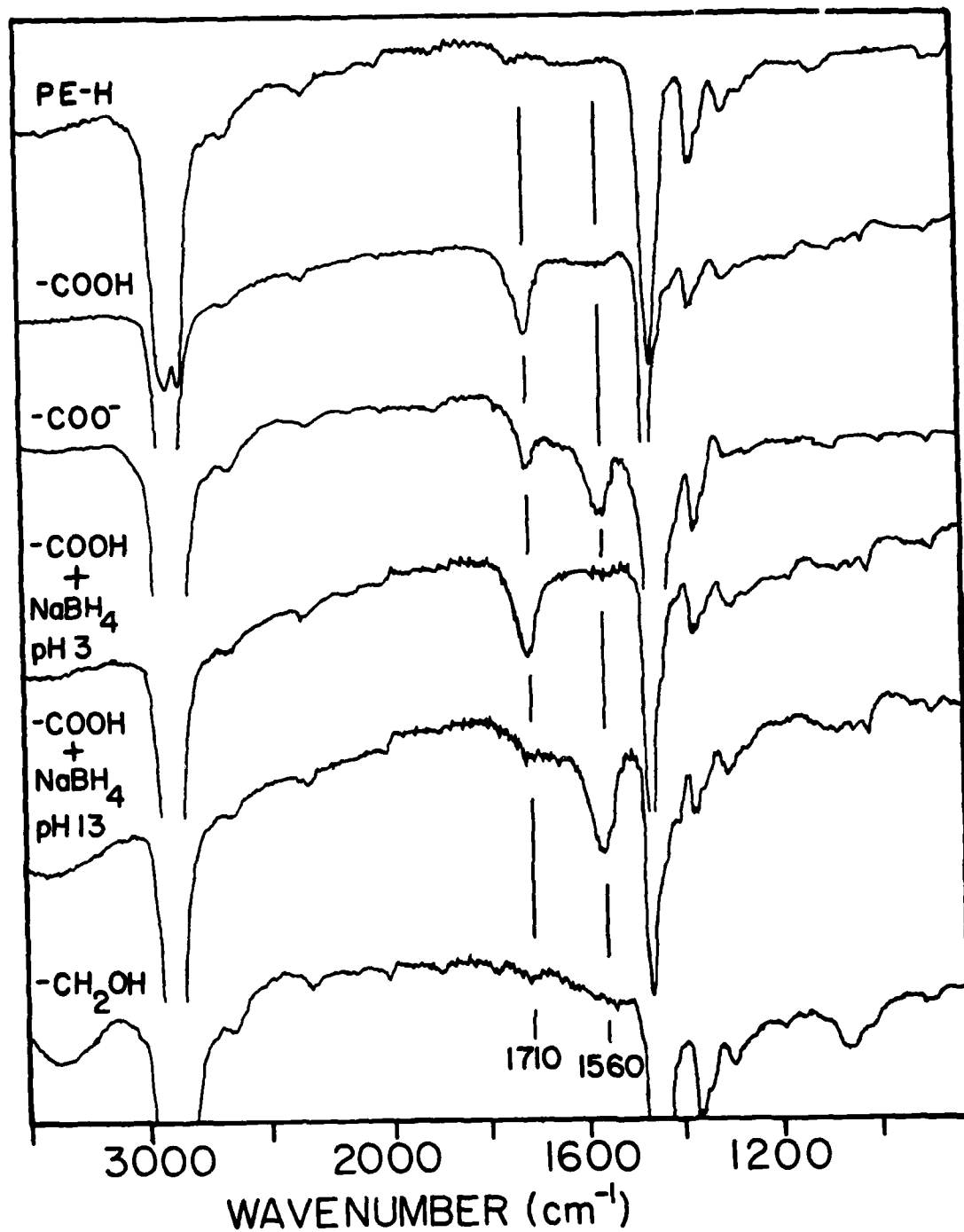


Figure 6. ATR-IR spectra of samples of polyethylene: following extraction (PE-H); after oxidation (PE-COOH); after treatment with 1 M NaOH (PE-COO⁻); following treatment with NaBH₄, shown after equilibration of the surface at pH 3 and at pH 13; and following treatment with 1 M BiH₃·THF (PE-CH₂OH).

as polyethylene carboxylic acid to emphasize the reactive character of the carboxylic acid groups.

Figure 7 gives ESCA survey spectra for representative samples of PE-H and PE-CO₂H and shows the magnifications of the regions of interest for PE-CO₂H. The only visible surface functionality is that containing oxygen. In particular no residual chromium, nitrogen, or sulfur-containing species are evident.³⁷ Sulfur containing species have been observed by others in samples of polyethylene oxidized with H₂SO₄/CrO₃ solutions.^{14,15} We attribute the absence of such species on our samples to the aqueous nature of our oxidizing medium compared to these others which were anhydrous¹⁵ or contained very little water.¹⁴

Density of Surface Functional Groups. We have measured the density of surface carboxylic acid groups using a number of techniques in previous studies.⁵ As a check, the surface carboxylic acid groups generated during the course of this work were measured using a chemical procedure: they were converted to glycy l amides by treatment with excess carbodiimide and N-hydroxysuccinimide followed by tritiated glycine (Scheme I). The sample was washed to remove excess glycine and, in a subsequent step, the glycine moieties were removed by acid hydrolysis. The density of carboxylic acid groups estimated by this procedure is $16 \times 10^{14} \text{ cm}^{-2}$. This number is in good agreement with estimates obtained using other techniques.³⁸

Interpretation of this surface density is complicated by two facts: First, at present, there is no reliable method for estimating the roughness of polyethylene or polyethylene carboxylic acid. Second, the thickness of the oxidized interfacial layer through which the carboxylic acids are distributed is not known. The measurement of surface density reported here is given in terms of "geometrical" rather than "true" surface areas: that is, it is not

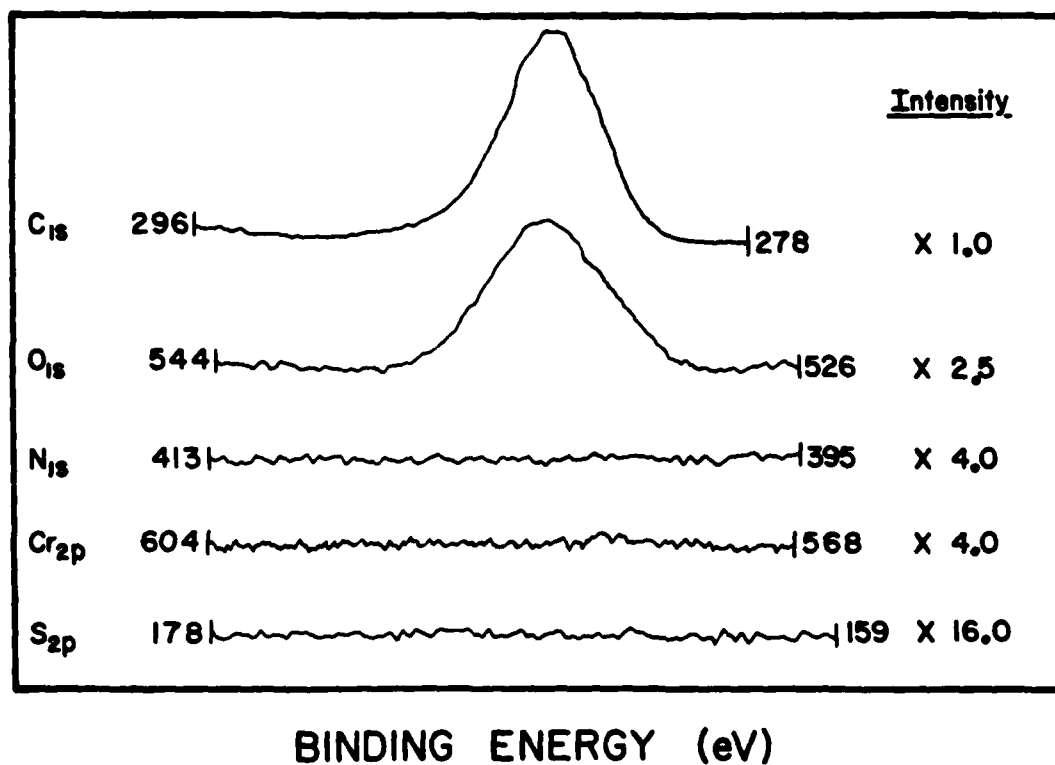
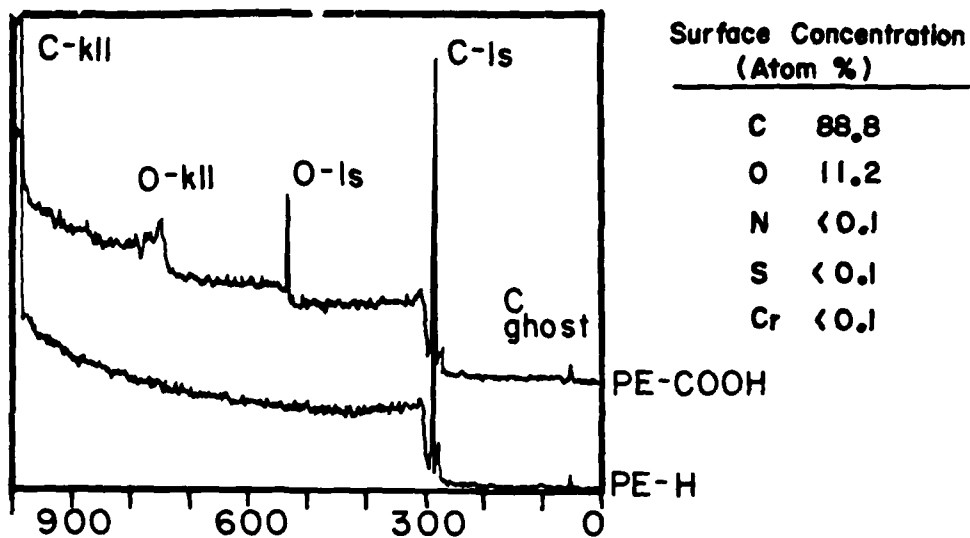


Figure 7. ESCA (XPS) survey spectra of unoxidized and oxidized polyethylene (top left) and the composition of the surface of PE-CO₂H (top right) determined by integrating the peaks obtained by analyzing only over the binding energies characteristic of elements of interest (bottom).³⁷

corrected for microscopic roughness of the surface. To our knowledge, no technique presently available is capable of measuring accurately the microscopic roughness of small samples of surfaces having low surface free energy (e.g. PE-H and PE-CO₂H). Examination of electron microscope photomicrographs is compatible with surface roughness factors of 2-3 (see below). The surface density of carboxylic acid groups in a close-packed monolayer (as in a stearic acid crystal or in a Langmuir-Blodgett monolayer)³³ is approximately $5 \times 10^{14} \text{ cm}^{-2}$. The carboxylic acid group density inferred for PE-CO₂H ($16 \times 10^{14} \text{ cm}^{-2}$ of geometrical film area) thus indicates a high density of these groups on the polymer surface, but the ambiguities resulting from uncertainties in the yields of the reactions used to estimate surface functional group concentrations, in the estimates of surface roughness, and in the information concerning the depth distribution of carboxylic acid and ketone groups in the interfacial region make it impossible, at present, to describe accurately the two-dimensional distribution of carboxylic acid groups on the exterior surface of this material. We note, however, that the reaction used to introduce carboxylic acid groups--oxidative cleavage of polyethylene chains--results in a material in which, at maximum, each polyethylene chain entering the surface region terminates in one CO₂H group. Thus, the maximum density of CO₂H groups in the interfacial region is fixed by the density of polyethylene chains in this region (Figure 8).

Surface Morphology: Scanning Electron Microscopy. Figure 9 comprises electron micrographs of unoxidized, lightly oxidized, and heavily oxidized samples of polyethylene. The lightly oxidized sample (oxidized for 60 sec, an interval that generates a surface whose hydrophilicity has reached its limiting value: Figure 4) has features like those of unoxidized polyethylene, although the contrast is greater. Both films resemble the surface of a can of

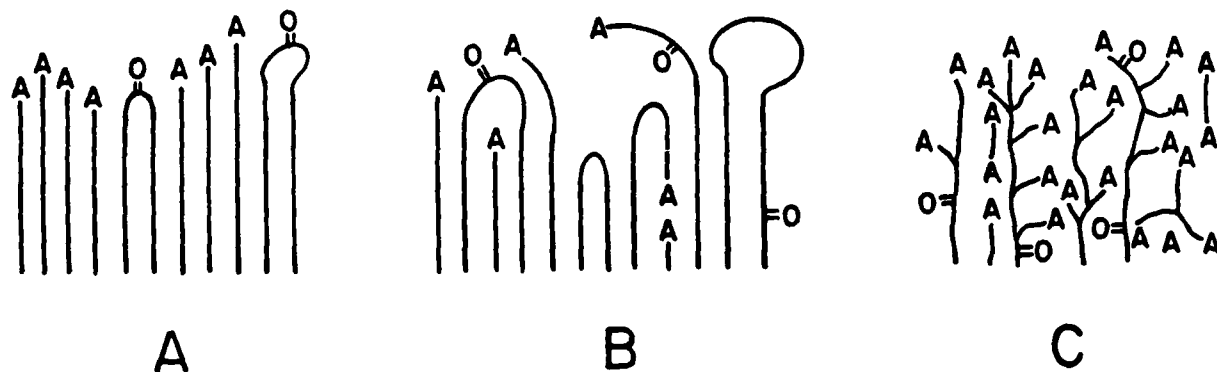


Figure 8. Schematic representations of possible structures of PE-CO₂H. In each, A = CO₂H, =O = ketone, and \sim = -(CH₂)_n-. Each is drawn as if the polyethylene chains entering the oxidized region were crystalline; the argument is not changed if they are amorphous. Model A represents a limit of surface oxidation. The surface is rough, but no acid groups exist in the interior of the polymer. B represents a more plausible model: the groups in contact with water are a mixture of carboxylic acid, ketone, and methylene groups. Oxidized moieties also are found in the subsurface region. Although two acid groups do not exist on a single short polyethylene chain, a ketone can exist on a chain terminated by an acid group. Model C cannot represent the surface. The oxidation reaction does not introduce oxidized groups as branches, and low molecular weight species would be lost from the material on rinsing with water.



PE-H

H

1 μm



60 sec oxidation



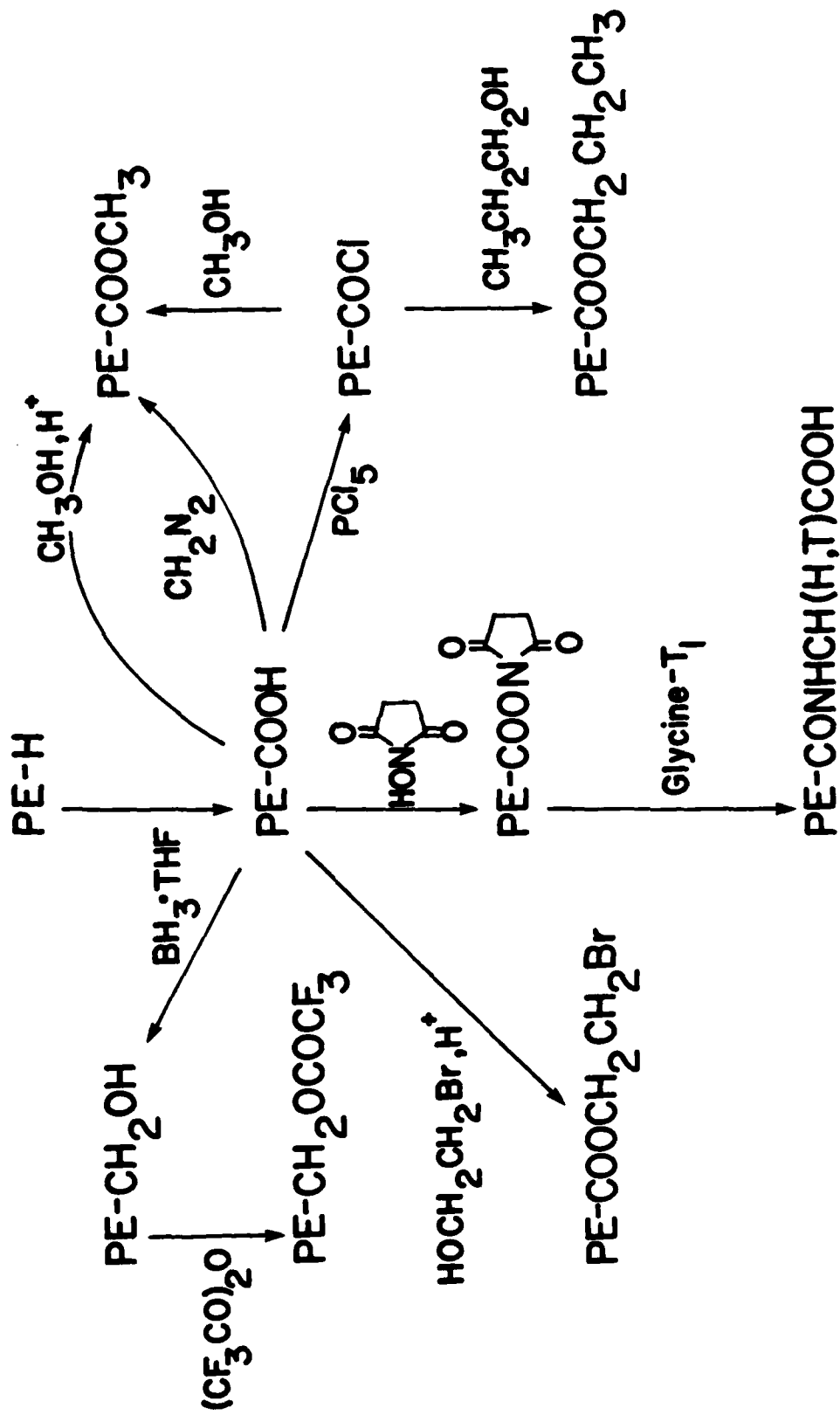
6 min oxidation

PE-COOH

Figure 9. SEM micrographs of unoxidized and oxidized polyethylene; the micrograph labeled "60 sec oxidation" is of a sample representative of those used in this work; that labeled "6 min oxidation" is more heavily etched. The films are coated with ~ 200 Å of Au/Pd (5% Pd).

worms. The features visible in the photomicrographs are believed to be crystalline lamellae.^{8,9} Because polyethylene is an insulator, it is necessary to coat the surface with a thin (200 Å) conducting layer before microscopic examination. Thus features smaller than ~200 Å cannot be discerned in these photomicrographs. Heavily oxidized polyethylene is heavily etched and looks like soggy cornflakes. The hydrophilicity (as measured using contact angles with water) and the chemical reactivity of the heavily and lightly etched surfaces are, however, indistinguishable. We have occasionally used heavily rather than lightly etched surfaces as substrates while developing techniques for synthetic modification of PE-CO₂H: the higher surface roughness and surface area of the heavily etched samples puts a larger number of functional groups in the region probed by ATR-IR, and thus increases the sensitivity of infrared spectroscopy in following functional group transformations. The reactivities of lightly and heavily etched samples seem to be indistinguishable.

Accessibility of Surface Functional Groups. One important reason for choosing to work with a surface containing carboxylic acid groups is that this functional group provides the basis for some of the most reliable and convenient functionalization procedures available in organic chemistry. During the course of this work we have prepared a substantial number of derivatives of PE-CO₂H; representative experimental procedures used to obtain these derivatives are summarized in Scheme I. Figure 10 summarizes ATR-IR spectra of the carbonyl region of the spectrum for samples of PE-CO₂H converted into the corresponding methyl ester PE-CO₂CH₃ (prepared by three independent procedures: treatment with diazomethane, acid-catalyzed esterification, and reaction of the acid chloride PE-COCl with methanol); the alcohol PE-CH₂OH (obtained by reaction of PE-CO₂H with BH₃·THF); and an acyl



Scheme I. Reactions used to convert the carboxylic acid groups of PE-CO₂H to derivatives.

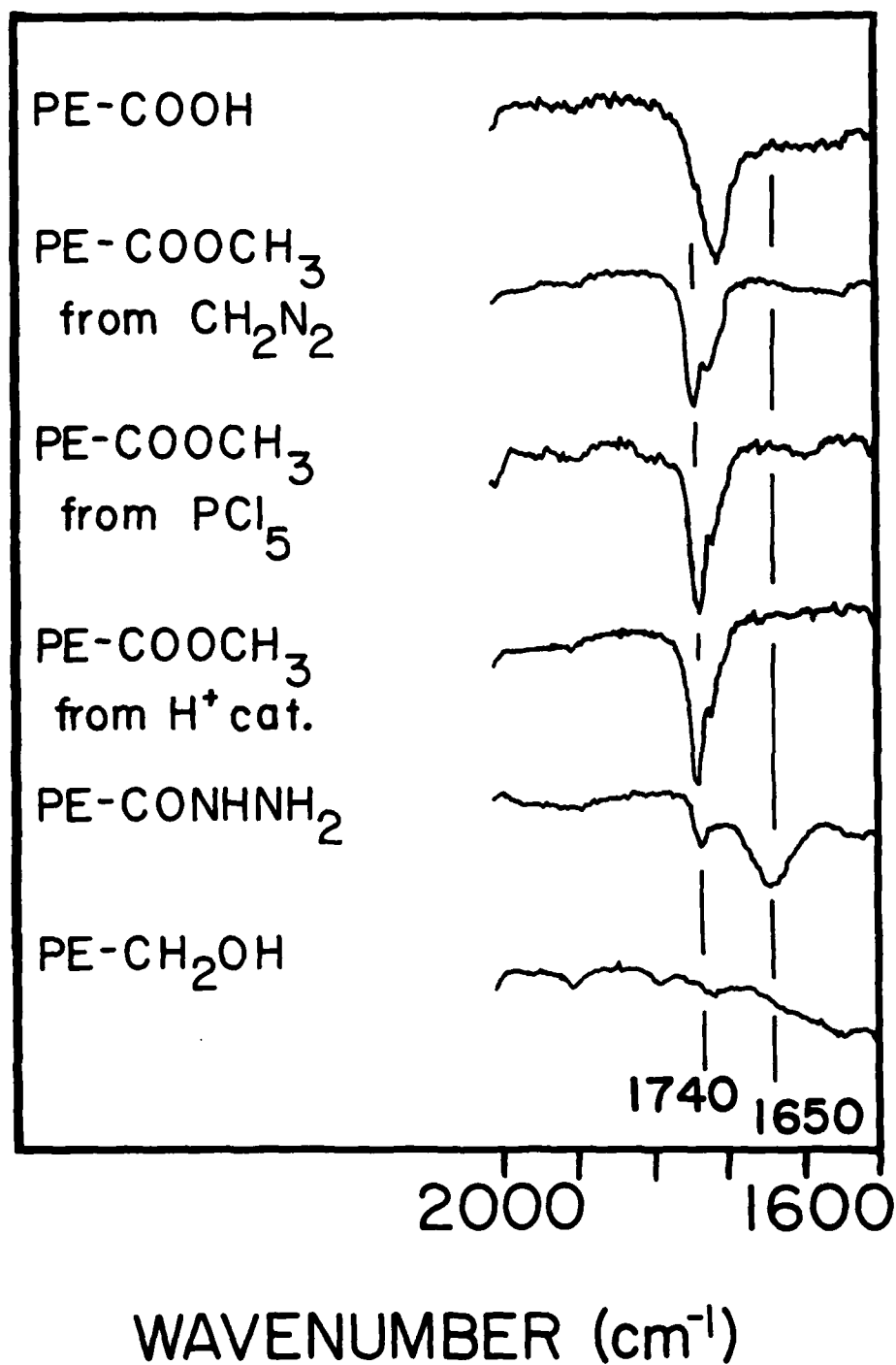


Figure 10. ATR-IR spectra of the carbonyl region of derivatives of PE-COOH.

hydrazide PE-CONHNH₂. The important conclusion from these spectra is that the derivatizing reactions proceed in high yield. It is difficult to estimate yields reliably for these procedures, especially because of the underlying absorption in the carbonyl region due to ketone functional groups. It is qualitatively evident, however, that the majority of the carboxylic acid groups are accessible to derivatizing reagents.

Figure 11 summarizes an alternative approach to following the course of derivatization of surface carboxylic acid groups on PE-CO₂H, using measurements of contact angle. This figure summarizes curves of contact angle vs pH obtained using unbuffered sessile drops for PE-CO₂H and for several of its derivatives that do not contain acidic groups. As indicated previously, the break at pH ≈ 10 in the curve for PE-CO₂H does not represent a pK_a; rather, it is a measure of the concentration of surface carboxylic acid groups. Corresponding curves for unfunctionalized polyethylene, for esters of PE-CO₂H, and for PE-CH₂OH³⁹ are also summarized in Figure 11. The important observation is that none of these derivatives of PE-CO₂H shows a break in the curves of θ_a vs pH. Derivatives having nonionizing surface groups, including PE-COOR (R = ethyl ($\theta_a = 106^\circ$), propyl ($\theta_a = 112^\circ$) and octyl ($\theta_a = 119^\circ$)) were made and showed no breaks in curves of θ_a vs pH.⁴⁰ If unreacted surface carboxylic acid groups remained in these samples, they should ionize on treatment with base; this ionization should result in a change in surface hydrophilicity, and thus in contact angle. The fact that no such change is observed suggests that the concentration of surface carboxylic acid groups is less in these samples than 10% of that in PE-CO₂H.⁴¹ The conclusion from this method of probing surface reactions is thus in good agreement with observations from ATR-IR: that is, the majority of surface CO₂H groups (probably more than 90%) are consumed in these derivitizing reactions.

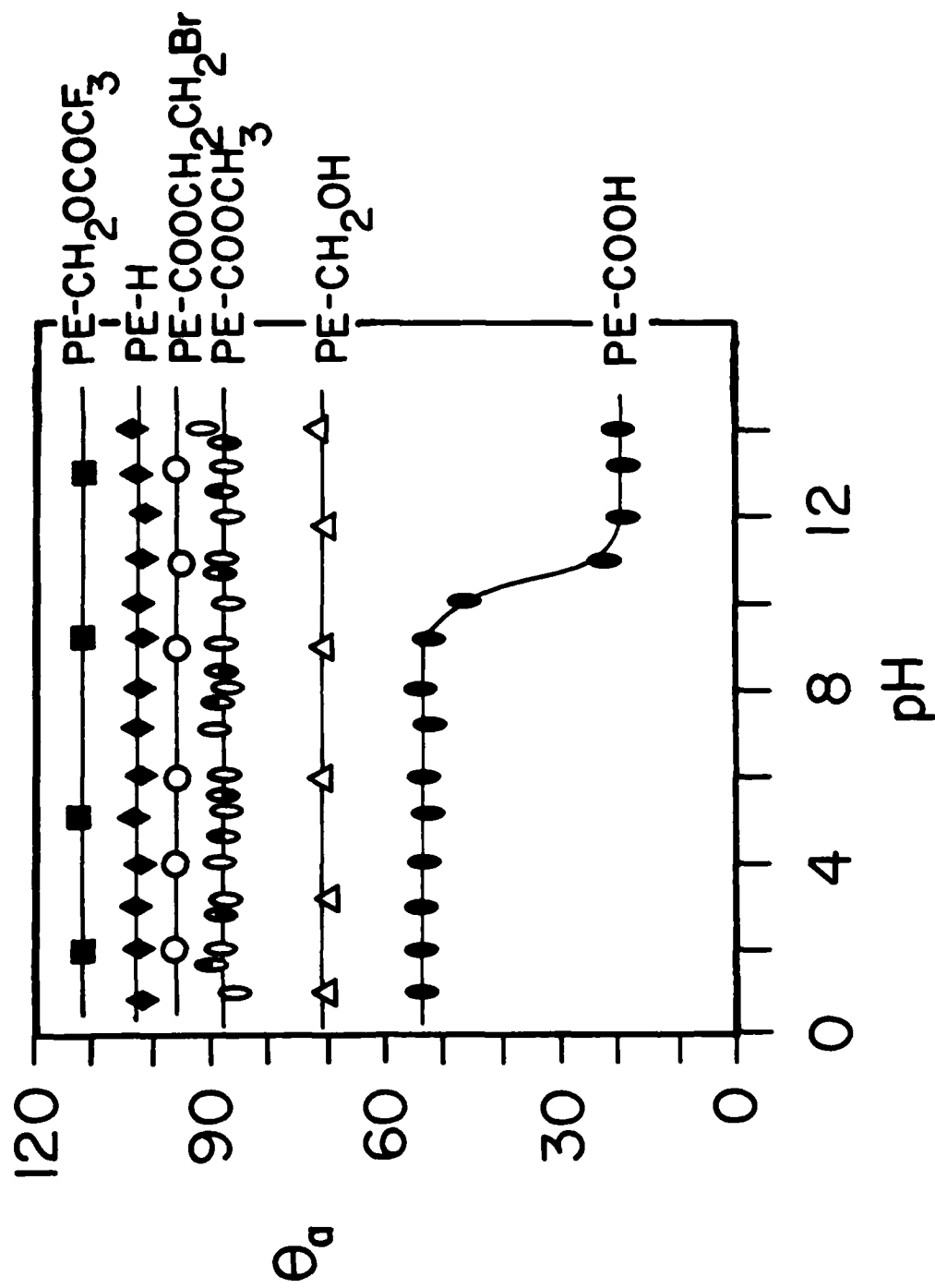


Figure 11. Dependence of θ_a on pH (unbuffered solutions; pH adjusted with NaOH or HCl) for PE-COOH and several derivatives. The PE-CO₂CH₃ samples were made as follows: ○, by acid-catalyzed esterification; ◐, by reaction with diazomethane; ● by reaction of PE-COCl and CH₃OH.

Acid-Base Reactions of PE-CO₂H

ATR-IR Titrations. One technique used to examine the extent of ionization of the surface carboxylic acid groups as a function of pH of the contacting solution was to measure the relative concentrations of carboxylic acid and carboxylate ions using infrared spectroscopy. These experiments were complicated by two difficulties. The first stems from the presence of two types of carbonyl groups on the surface: ionizable carboxylic acids and nonionizable ketones. The second stems from intrinsic experimental difficulties due to the requirement that PE-CO₂H (PE-CO₂⁻) samples be reasonably dry when placed in contact with the ATR-IR plate, in order to obtain usable spectra and to avoid damaging the plate.

The PE-CO₂H films were equilibrated with an excess of buffered water (0.01 M phosphate, or organic buffer if specified) at a given pH. No particular interval was used to effect these equilibrations: we assume that they are rapid (<1 min). The film was removed from the aqueous solution, and excess water removed by brief blotting using a piece of filter paper. Initial experiments indicated that traces of acid or base on the filter paper were sufficient to change the pH of the residual aqueous film on the surface of the polyethylene carboxylic acid, and thus to change the apparent extent of ionization of the surface carboxylic acid groups in an irreproducible way. To circumvent this difficulty, we developed a technique in which the filter papers used in blotting were themselves prepared: The filter paper was equilibrated with a buffered aqueous solution (0.01 M phosphate or organic buffer), and then dried in an oven. Use of these buffered filter papers led to highly reproducible results. Following blotting to remove all visible water from the surface of the PE-CO₂H (PE-CO₂⁻), the polyethylene films were

dried briefly under vacuum (60 min, 0.01 torr); and then examined by standard ATR-IR techniques.

One can imagine that this technique might result in serious artifacts: contamination of the surface with concentrated buffer, reaction of surface functionality with components of the atmosphere during handling, reaction with traces of acid or base present on the surface of the ATR-IR plates. It is impossible to exclude influences on the results due to these types of processes. We note, however, that the data obtained using this procedure are in excellent agreement with those obtained by completely independent procedures based on measurements of contact angle as a function of pH, and in reasonable agreement with direct titration of suspensions of surface-oxidized granular polyethylene (see below). This agreement provides strong support for the belief that the infrared procedure using buffered filter paper to remove excess water provides reliable and accurate data.

Figure 12 shows representative ATR-IR spectra in the carbonyl region as a function of the pH of the aqueous solution used. The frequency (1560 cm^{-1}) at which carboxylate absorption falls is relatively unobscured in PE-CO₂H; we assume that the residual absorption at 1710 cm^{-1} in the spectrum obtained at pH 13 is due to ketone groups. The transmission spectra obtained were converted by computer to absorption spectra and the ratio of the absorbance at 1560 cm^{-1} to the total absorbance at 1710 cm^{-1} and 1560 cm^{-1} was determined for each pH (eq 8).

$$\underline{R}(\text{pH}) = \frac{A_{1560}(\text{pH})}{A_{1710}(\text{pH}) + A_{1560}(\text{pH})} \quad (8)$$

Equation 9 relates the observed ratios $\underline{R}(\text{pH})$ to the extent of ionization at each value of pH using the ratios obtained at pH 1 (CO₂H) and pH 13 (CO₂⁻) to

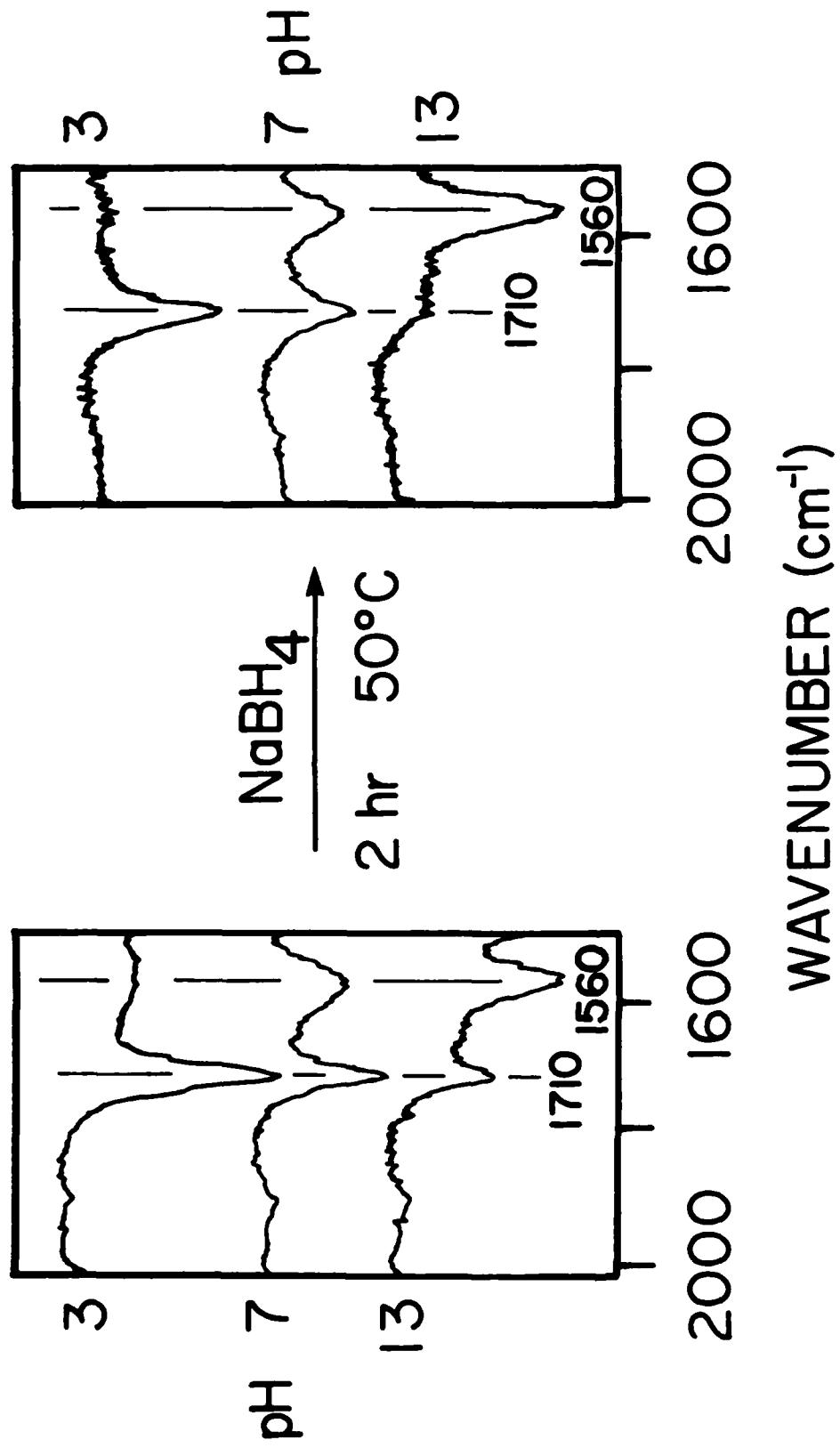


Figure 12. ATR-IR spectra of PE-COOH (left) and PE-CO₂H after treatment with NaBH₄ to remove ketone and aldehyde functionality (right) at several values of pH.

set the endpoints of the titration ($\alpha_i = 0$ and $\alpha_i = 1$ respectively; eq 9).

$$\alpha_i(\text{pH}) = \frac{\underline{R}(\text{pH}) - \underline{R}(\text{pH } 1)}{\underline{R}(\text{pH } 13) - \underline{R}(\text{pH } 1)} \quad (9)$$

In this equation $\underline{R}(\text{pH } 1)$ is used as a small baseline correction for any absorbance at 1560 cm^{-1} in a sample in which the carboxylic acid groups are completely protonated and $\underline{R}(\text{pH } 13)$ is less than 1 due to ketone absorbance at 1710 cm^{-1} . The assumption that the absorption at 1710 cm^{-1} is due to ketone is supported by spectra taken of PE-CO₂H that has been treated with borohydride ion. We expect this treatment to reduce ketone and aldehyde groups, but to leave carboxylic acid groups intact.⁴² ATR-IR spectra taken on such a sample (Figure 12, right) support this hypothesis. The undesired absorption at 1710 cm^{-1} has been much reduced in intensity; the other spectral features of the sample, especially its dependence on pH, remain the same.

Figure 13 summarizes values of the extent of ionization α_i obtained using ATR-IR spectroscopy as a function of pH for PE-CO₂H (and, for comparison, for acetic acid⁴³ and polyacrylic acid⁴⁴). The cross-hatched oval at pH 8 contains data determined using seven different buffers⁴⁵; the agreement among these data indicates that specific buffer effects are not important. This curve has two interesting characteristics: First, its width is significantly greater than that of CH₃CO₂H, and is qualitatively similar to that of polyacrylic acid. Second, the extrapolated value of $\alpha_i = 0$ ($\text{pK}_a \sim 6$) is one to two pK_a units less acidic than acetic or polyacrylic acids. The width is compatible with at least two hypotheses concerning the character of the carboxylic acid groups of PE-CO₂H: either they comprise a heterogeneous population with a range of values of pK_a , or they are a homogeneous population that acts as a polybasic acid. The high value of the initial pK_a suggests, as

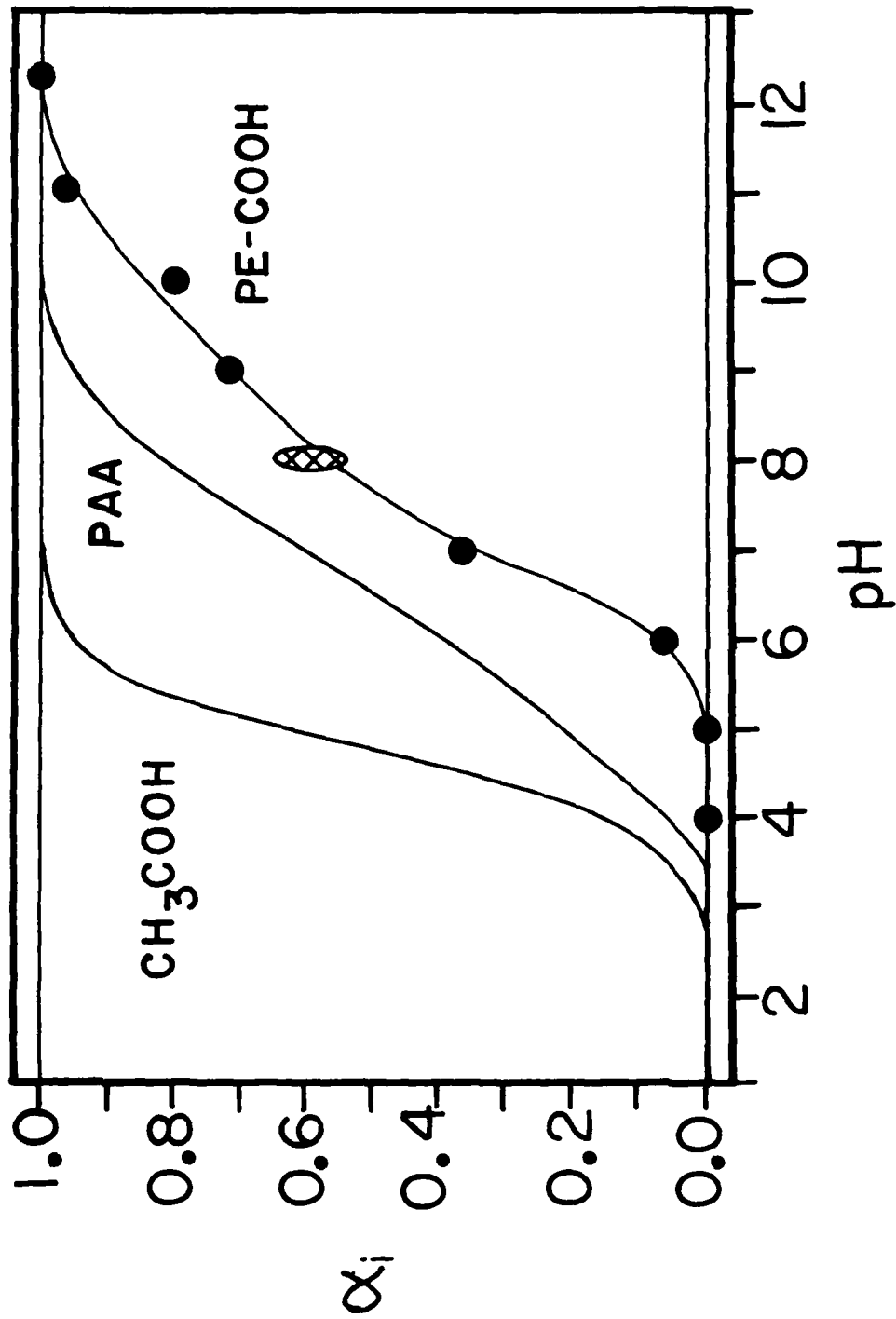


Figure 13. Extent of ionization α_i (eq 3) obtained for PE-CO₂H as a function of pH using ATR-IR spectroscopy. The experimental points are taken from the types of experiments summarized in Figure 12 using eq 8 and 9. The cross-hatched oval at pH 8 contains the data points determined using seven buffers (0.01 M).⁴⁵ Other curves shown are for acetic acid⁴³ and polyacrylic acid (PAA).⁴⁴

one additional hypothesis, that solvation of the carboxylate ions of PE-CO_2^- is relatively poor. We defer further discussion of these values until after presentation of data derived from measurements of contact angle and from direct potentiometric titration.

Titration by Contact Angle. All measurements of contact angle for water on $\text{PE-CO}_2\text{H}$ and $\text{UHMW-CO}_2\text{H}$ as a function of pH were obtained using sessile drop techniques. Values of the contact angle were determined visually, estimating the tangent of the curve to the water drop at the point of intersection with the surface. This procedure is inexact, but reproducible. Almost all of the work reported in this section was obtained using 1- μL drops in an atmosphere having 100% relative humidity. The size of the drop influences the measured value of contact angle for small drops,¹⁶ but we did not systematically explore the relation between the size of the drop used and the observed contact angle, other than to establish that θ_a was relatively insensitive to this parameter.

Most of our work has involved measurements of θ_a , the "advancing" contact angle.⁴⁶ Both PE-H and $\text{PE-CO}_2\text{H}$ show large contact angle hysteresis. The receding contact angles on PE-H (75°) and $\text{PE-CO}_2\text{H}$ ($< 5^\circ$) are significantly lower than the advancing angles (103° and 55° respectively). The origin of this hysteresis is probably some combination of surface roughness and swelling of the outermost region of the polymer (a few \AA perhaps) by the drop. The very low values of receding contact angle for $\text{PE-CO}_2\text{H}$ precluded the use of inverted bubble methods for measuring contact angle. Figure 14 summarizes the measured value of θ_a as a function of the interval between the application of the drop to the surface and the measurement. These data emphasize the importance of control over humidity: in low-humidity atmospheres, evaporation of water from the small drop leads to serious drift in the measured value of

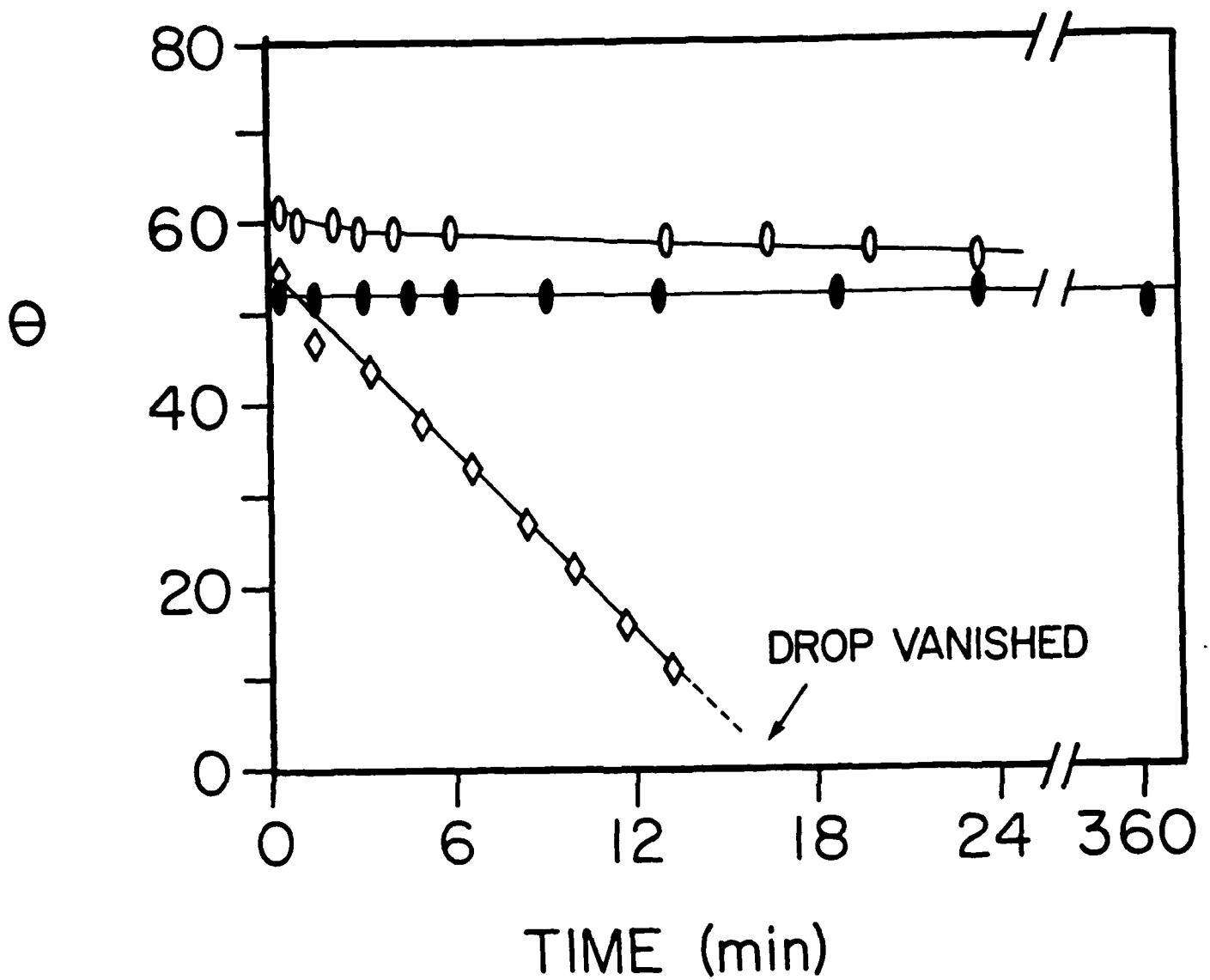


Figure 14. Variation in the measured value of θ as a function of the interval between application of the drop to the surface and the measurement. Data points are for typical single drops; ●, applied and measured under air saturated with water vapor (100% relative humidity); ○, applied at ambient humidity and then raised to 100% relative humidity; ◇, applied and kept at ambient humidity.

contact angle. The drop is stable at 100% humidity. A brief survey indicated that changes in temperature have relatively small influences on θ_a ($T < 40$ °C). The past history of the PE-CO₂H also has only a small influence on the measured value of θ_a . In particular, there seem to be no important influences due to slow hydration of the sample (a factor which might be important either in determining surface structure, or in determining γ_{SV}).

We believe that the contact angle measurements reported in this section are reproducible $\pm 3^\circ$ over the range of values of pH examined (reproducibility and accuracy become less at values of θ less than 15°). It is difficult to measure reproducibility in a well-defined way: applying multiple drops of liquid to the same spot on the film is technically impractical. Repeated measurements taken over the surface of the film indicate, however, that the value of θ_a does not vary with the location of the drop on the film. The measured curves relating θ_a and pH are also reproducible. Figure 15 summarizes data obtained from several films: a dry film; a film initially equilibrated at pH 13 for several hours, then rinsed in distilled water and dried briefly in air; a film equilibrated similarly at pH 1; and a film repeatedly cycled between pH 1 and pH 13. All of these films give indistinguishable results.

The dependence of θ_a on pH for water on UHMW-CO₂H is similar to that for PE-CO₂H (Figure 15), although the surface of UHMW-CO₂H at low values of pH is consistently slightly more hydrophilic than that of PE-CO₂H, and is slightly less hydrophilic at high values of pH. These observations suggest that UHMW-CO₂H may have a lower density of surface carboxylic acid groups than PE-CO₂H, as well as some nonionizable polar surface functionality, not present (or not present in as high concentration) on PE-CO₂H which contributes to the low

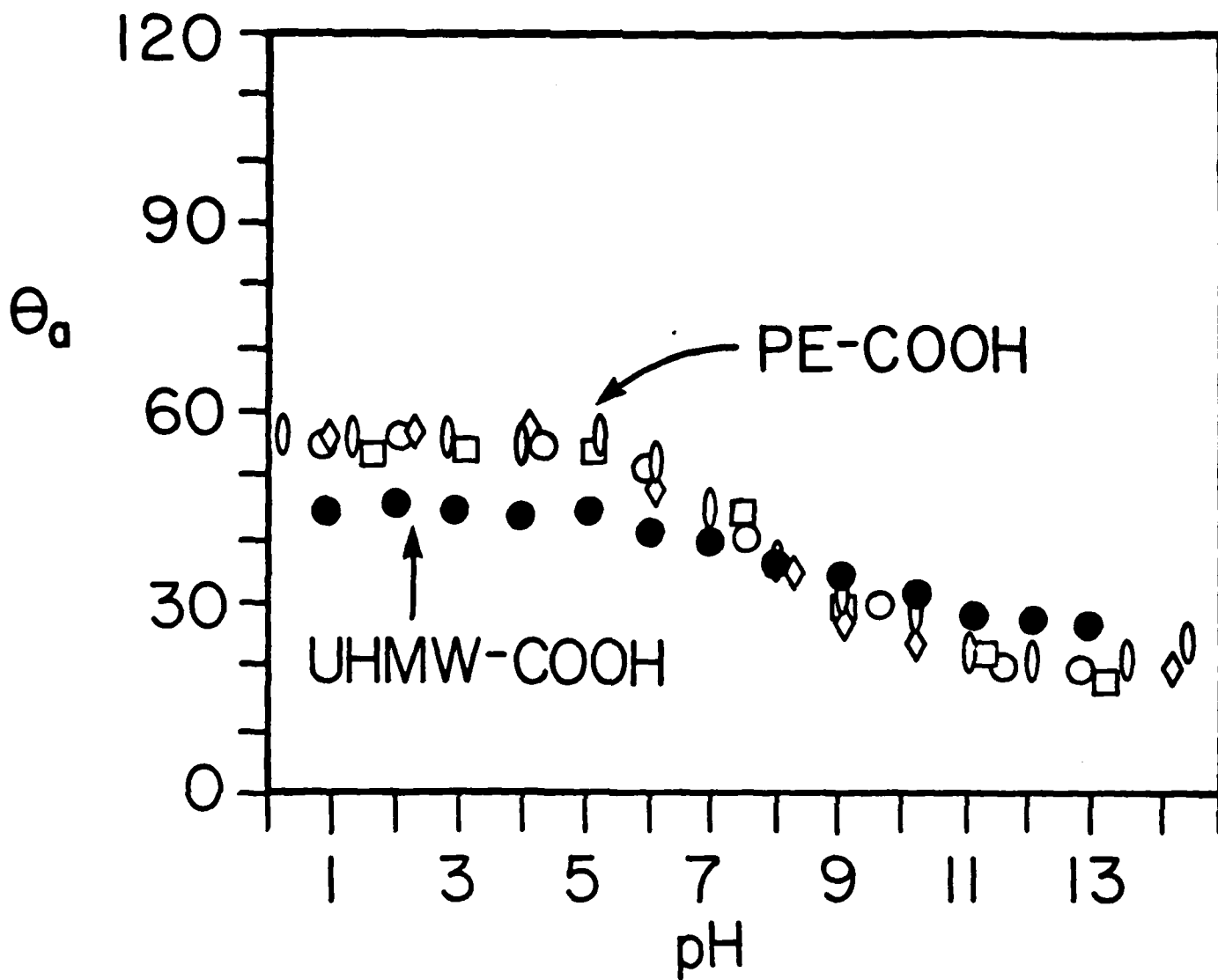


Figure 15. Dependence of θ_a on pH for PE-CO₂H with various pretreatments: ○, dry film; □, film equilibrated at pH 13 (NaOH) for 3 h, then washed in distilled water for 5 min, and dried in air for 30 min; ◇, film equilibrated at pH 1 (HCl) for 3 h, then washed and dried as above; ○, film subjected to five cycles between pH 1 and pH 13 (5 min each) then washed in distilled water for 5 min and dried. The results for UHMW-CO₂H (no pretreatment) are included (●).

value of θ_a at low pH. We have not characterized the surface functionality on UHMW-CO₂H, and do not speculate on the nature of the non-CO₂H functionality.

We indicated in the Introduction that the most important technical problem that required solution in exploring the pH dependence of θ_a (that is, the hydrophilicity of the surface) on the pH of the aqueous solution was that of avoiding experimental artifacts due to the high surface density of carboxylic acid groups present on PE-CO₂H. In experiments in which the surface of PE-CO₂H was in contact with a drop of unbuffered water, the number of surface carboxylic acid groups on the surface was, as indicated, greater than the number of hydroxide ions present in solution for values of pH <10. To circumvent this problem we have, in general, used buffered aqueous solutions.⁴⁷ Figure 16 contrasts the dependence of θ_a (obtained using sessile drop techniques) on pH for three systems: unbuffered aqueous solutions; aqueous solutions buffered with phosphate ion; and aqueous solutions buffered with organic buffers. For PE-CO₂H, it is clear that buffered systems provide similar experimental curves; unbuffered drop experiments are different. We assumed in deriving eq 6 that θ_a depends only on the extent of ionization of surface carboxylic acid groups. Particularly in systems incorporating organic buffers, the correctness of this assumption is not obvious a priori. Figure 16 contains a point (shown as a crosshatched ellipse at pH 8) which includes the value of θ_a obtained with five different organic buffers and phosphate buffer.⁴⁸ The independence of θ_a on the buffer used indicates that the observed trends in θ vs pH are independent of buffer structure. The close similarity between the several types of buffered systems suggest that these systems are free of the influence of partial neutralization of the aqueous phase by the surface carboxylic acid groups, and indicate that the

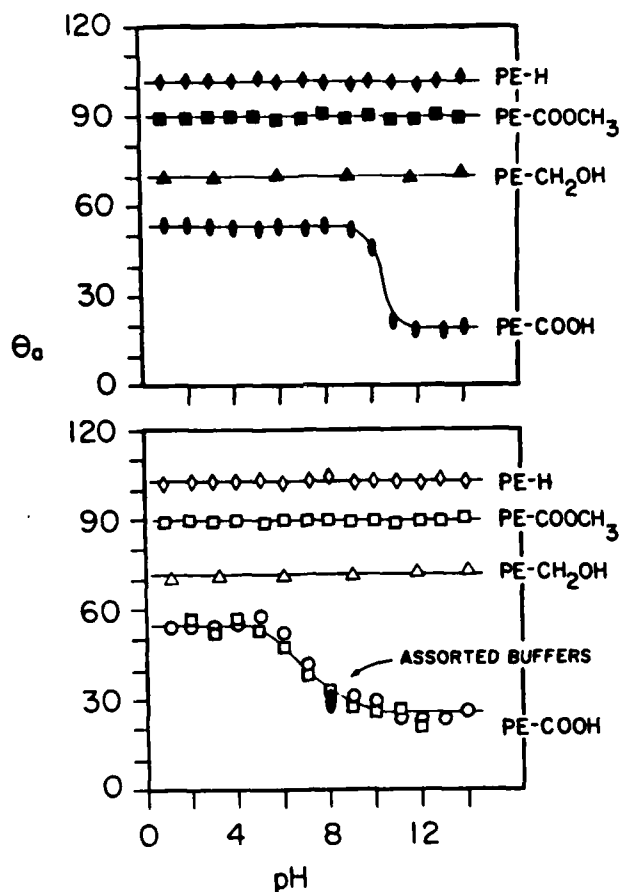


Figure 16. Dependence of θ_a on pH for surface functionalized of polyethylenes. Top: Using unbuffered aqueous solutions (pH adjusted with NaOH or HCl). Bottom: Using buffered aqueous solutions.⁴⁵ Buffers used: \square , 0.1 M phosphate buffer; \circ , all others (0.05 M) as follows: pH 1, 0.1 N HCl; pH 2, maleic acid; pH 3, tartaric acid; pH 4, succinic acid; pH 5, acetic acid; pH 6, maleic acid; pH 7 and pH 8, HEPES; pH 9 and pH 10, CHES; pH 11, triethylamine; pH 12, phosphate; pH 13, 0.1 N NaOH. The cross-hatched oval labeled "assorted buffers" at pH 8 includes data for phosphate, MOPS, HEPES, TAPS, TRIS, triethanolamine.

experimental results are not influenced by buffer components acting as surfactants.

Figure 16 also includes measurements of θ_a as a function of pH for three systems (PE-H, PE-CH₂OH, PE-CO₂CH₃) that do not contain functional groups ionizable over the pH range of interest for PE-CO₂H. For all of these derivatives of polyethylene, θ_a is independent of pH within the limits of our experimental measurement. This independence supports the assumption that the curve obtained for PE-CO₂H reflects primarily a change in γ_{LS} due to conversion of carboxylic acid to carboxylate groups at high pH, and suggests that changes in γ_{LV} and γ_{SV} are unimportant over the pH range examined.²⁹

Figure 17 shows the dependence of curves of θ_a vs pH for PE-CO₂H on the strength of the buffer used. These curves demonstrate clearly the necessity of using buffers that have capacity sufficient to eliminate the influence of the surface carboxylic acid groups on the pH of the drop. It is difficult to calculate exactly the effective concentration of surface groups under a 1- μ L drop because it is a function of the shape of the drop (i.e. it is a function of θ ; eq 7), the surface roughness, and the density of surface groups. Using the measured values for PE-CO₂H and the curve of Figure 3, we estimate that the effective concentration of CO₂H groups ranges from ~ 0.1 mM at $\theta = 55^\circ$ to ~ 0.2 mM at $\theta \approx 22^\circ$. The capacity of the buffer appears to be adequate at 50 mM and begins to break down at 5 mM; at 0.5 mM the buffer is clearly being overwhelmed. Since buffering capacity is approximately half the buffer concentration (in either direction from the pK_a of the buffer) the buffering effect breaks down at approximately the concentration expected from independent estimates of the surface density of CO₂H groups on PE-CO₂H combined with calculated areas of drop coverage.

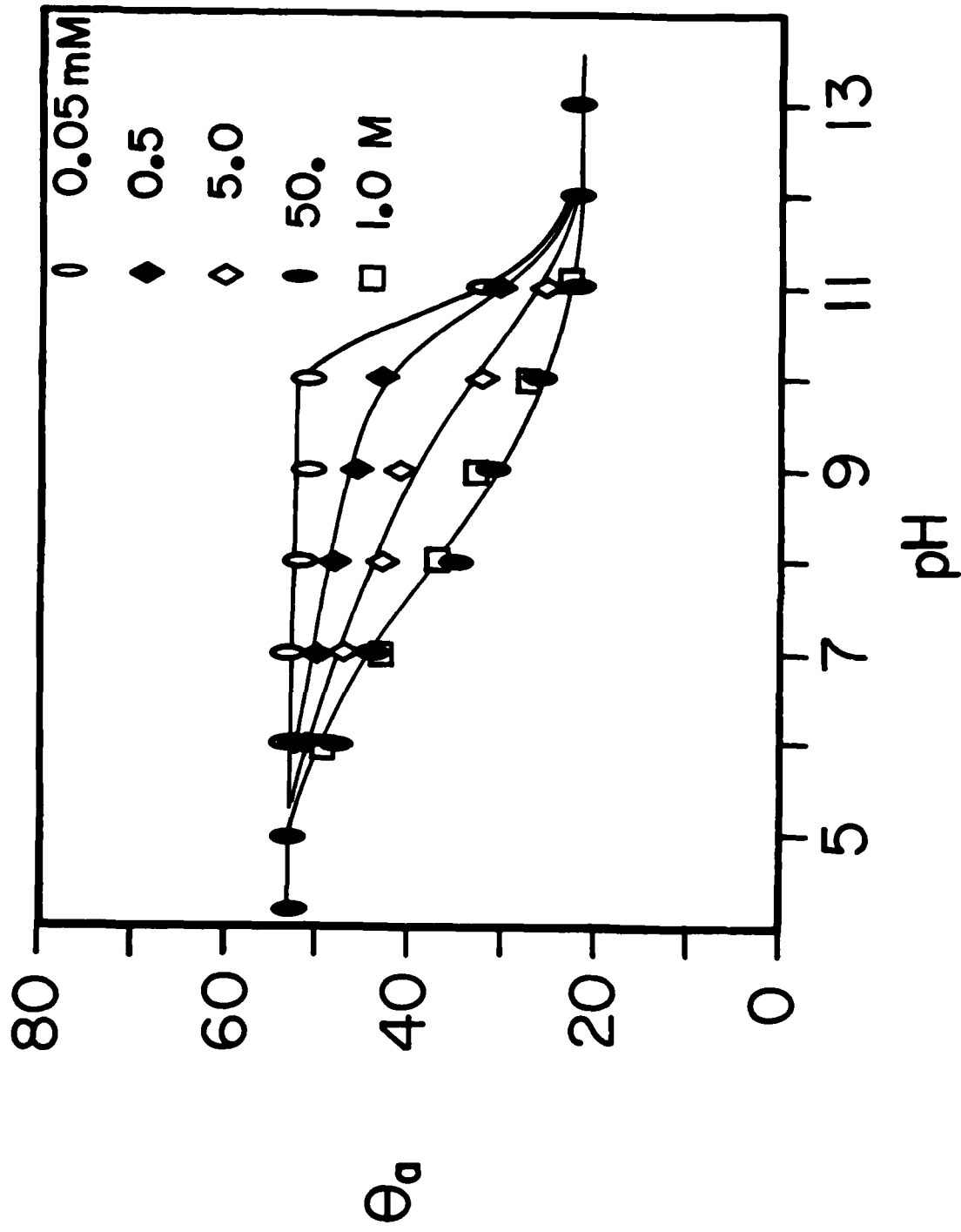


Figure 17. Dependence of θ_a on pH using different buffer concentrations on PE-CO₂H. Buffers used are the same as Figure 16 except at 1.0 M where liquid/vapor surface tension changes and ionic strength effects on θ_a can be significant. At 1.0 M the following buffers were substituted: pH 6 and pH 7, ethylenediamine; pH 8, Tris; pH 9 and pH 10, glycine; pH 11, γ -aminobutyric acid.

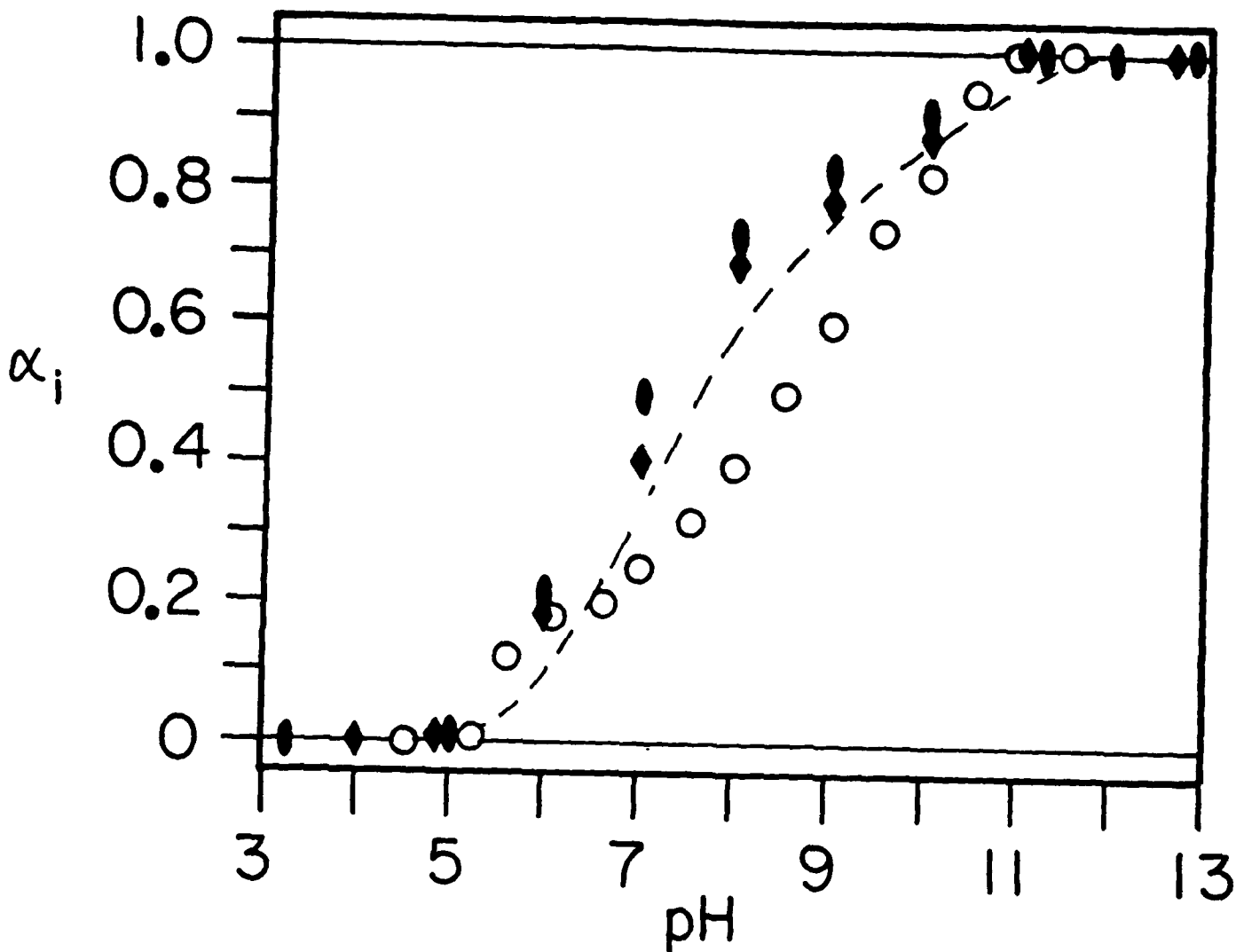


Figure 18. Extent of ionization, α_i , as a function of pH for PE-CO₂H: \bullet , using phosphate buffer; \blacklozenge , using organic buffers. The dashed line summarizes the ATR-IR data from Figure 13 for comparison. Data obtained by direct potentiometric titration of granular PE-CO₂H, \circ , are also shown.

From the data of Figure 16 we obtain a curve (Figure 18) relating the extent of ionization α_i to the pH for PE-CO₂H using eq 6. The dashed line in this figure represents the data obtained by ATR-IR; the good agreement between the data obtained from contact angle measurements and infrared spectroscopy supports the reliability of both techniques.

Direct Potentiometric Titration. There are too few carboxylic acid groups on a sample of PE-CO₂H film or UHMW-CO₂H sheet to titrate potentiometrically using the types of glass electrodes and pH meters available to us. There are, however, two systems with high enough surface area to permit direct titration. The first involves oxidized low density polyethylene granules (particle size \approx 0.3 mm). The second involves oxidized UHMW polyethylene chips prepared from UHMW sheet by cutting. Both the granules and the chips were oxidized by suspending in chromic acid solution for 5 minutes under the same conditions used to oxidize the flat samples.

Although the surface morphology of the granules and the chips are both certainly different than that of the low density film, we expect the acid-base behavior of carboxylic acid groups on the several systems to be comparable.

The direct potentiometric titration was performed by suspending the granular PE-CO₂H (or UHMW-CO₂H chips) in acidic water (pH 3) and back titrating with base; similar results were obtained by proceeding from basic to acidic media. Comparison with a similar titration in the absence of oxidized polyethylene permitted calculation of α_i as a function of pH using eq 10.

$$\alpha_i(\text{pH}) = \frac{(B^{\text{PE-CO}_2\text{H}} - B^{\text{H}_2\text{O}})_{\text{pH}}}{(B^{\text{PE-CO}_2\text{H}} - B^{\text{H}_2\text{O}})_{\text{pH} = 12}} \quad (10)$$

In this equation, for example, $B^{\text{PE-CO}_2\text{H}}_{\text{pH}}$ is the quantity of base added to the suspension of UHMW-CO₂H to reach the indicated value of pH. Results are

summarized in Figure 19, together with similar data from UHMW-CO₂H sheet obtained using contact angle data (e.g. Figure 15). The close similarity of the curves of α_i vs pH curves for UHMW-CO₂H in Figure 19 allows the following important observation: the fact that potentiometric titration and titration by contact angle yield indistinguishable curves provides strong support for the reliability of contact angle in measuring populations of surface groups (that is, for the correctness of eq 1 and 6), since each curve is reproduced in two independent experimental titration methods (potentiometric and contact angle for UHMW-CO₂H; ATR-IR and contact angle for PE-CO₂H). Further the slight difference observed between the titration curves for UHMW-CO₂H and PE-CO₂H is probably a valid reflection of differences in these materials rather than an artifact of the methods of measurement.

Similar titrations carried out on low density polyethylene granules gave similar results (Figure 20). In an additional check, we converted granular PE-CO₂H to granular PE-CO₂CH₃ by acid-catalyzed esterification. This material had no titrable groups. Upon hydrolysis to regenerate granular PE-CO₂H the original behavior was regained (Figure 20). The figure also shows the titration of granular PE-CO₂H in 0.1 M NaCl: no salt effect is observed.

These results on granular PE-CO₂H also allow two important observations. First, the fact that the titration curves are indistinguishable for granular PE-CO₂H as originally formed by oxidation and as regenerated from granular PE-CO₂CH₃ suggests that the titration curves obtained reflect the behavior of carboxylic acid groups only and that the conditions used in esterification and saponification do not induce irreversible reconstruction in the polymer surface. Second, the absence of a significant salt effect on the potentiometric titration curves supports similar observations made using

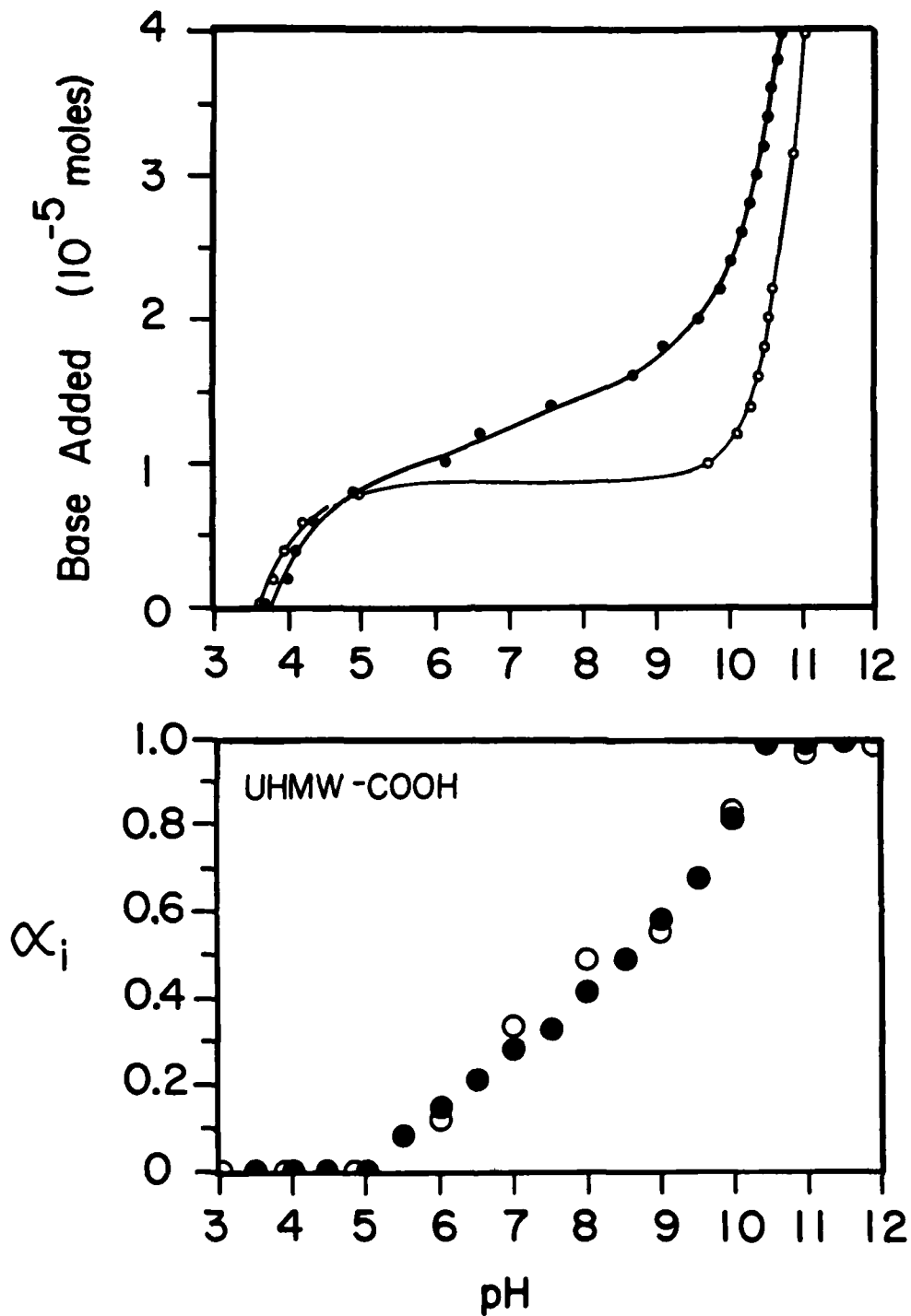


Figure 19. Top: Dependence of pH of UHMW-CO₂H suspended in water (●) and of water alone (○) as a function of added 0.1 N NaOH.

Bottom: Ionization (α_i) of UHMW-CO₂H as a function of pH:

● , determined from the data in the upper part of this Figure using eq 10 for UHMW-CO₂H chips; ○ , determined from changes in θ_a with pH (Figure 15) for UHMW-CO₂H sheet.

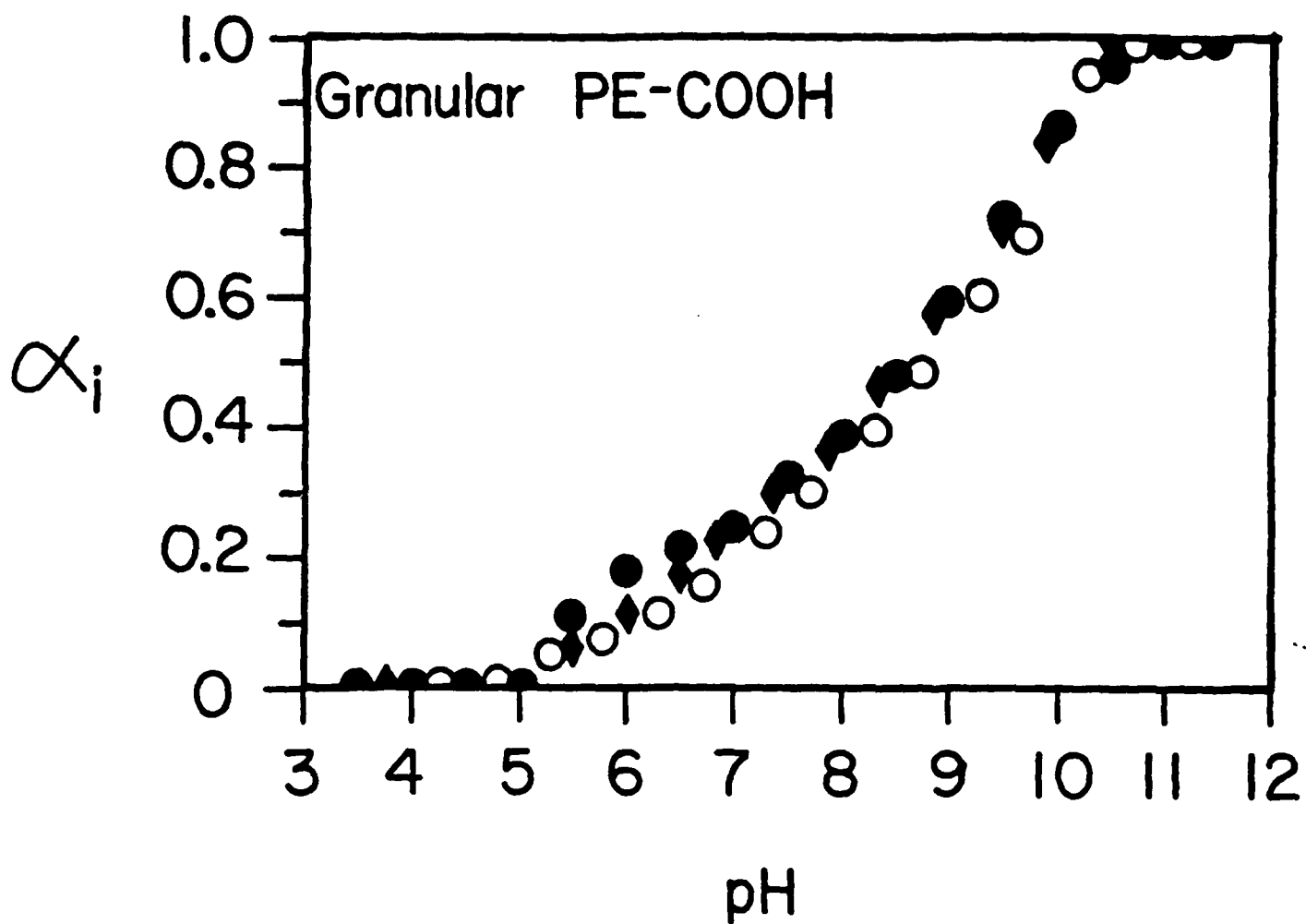


Figure 20. Ionization (α_i) determined by direct potentiometric titration as a function of pH for: ●, granular PE-CO₂H; ○, granular PE-CO₂H derived from hydrolyzed granular PE-CO₂OCH₃; ◆, granular PE-CO₂H in the presence of 0.1 M NaCl.

titrations by contact angle (see below) and is important in rationalizing the character of the surface carboxylic acid groups.

~~Effective pK_a .~~ A useful alternative presentation of the data summarized in Figure 18 is given in Figure 21. This figure plots the effective pK_a (pK_a^{eff} , eq 11) as a function of α_i . This equation relates the extent of

$$pK_a^{eff} = pH - \log\left(\frac{\alpha_i}{1 - \alpha_i}\right) \quad (11)$$

ionization α_i at a particular value of pH to the "effective pK_a " of the system: that is, to the value of pK_a which would be attributable to that extent of ionization for a simple monobasic acid. For a monobasic acid, pK_a^{eff} is independent of α_i . For a polybasic acid (PAA) pK_a^{eff} increases with α_i , reflecting the decreasing acidity of the remaining CO_2H groups as CO_2^- groups appear. Values of pK_a^{eff} are particularly relevant to the interpretation of behavior of a number of types of biological systems (especially cells), organized molecular assemblies (Langmuir-Blodgett films, micelles)^{49,50} and colloids.⁵¹ In many of these systems it is possible to measure the change in some physical property--electrophoretic mobility, solubility, surface charge-- as a function of pH. From these measurements, values of pK_a have been inferred for carboxylic acid groups which range from 3-11, and a certain amount of discussion has been devoted to rationalizing these differing values of pK_a .⁵²⁻⁶⁸ Figure 21 makes it clear that the term " pK_a " should be carefully defined in these discussions.

For PE- CO_2H , pK_a^{eff} increases with increasing α_i . As indicated above, this increase might, in principle, reflect either a change in the ease of ionization of a homogeneous population of carboxylic acid groups as the electrically neutral carboxylic acid groups are converted to anionic

carboxylate groups or heterogeneity in the population of carboxylic acid groups being examined.⁶⁹ The data in Figure 21 do not resolve this issue. We note, however, that the form of the dependence of pK_a^{eff} on α_j is quite different for PE-CO₂H and PAA. Thus, if electrostatic interactions within a homogeneous population of carboxylic acid groups is the dominant influence in PE-CO₂H (as it is believed to be in PAA), these systems must differ significantly in detail.

The results obtained for the ionization behavior of PE-CO₂H are in agreement with related results obtained by others. In particular, the $pK_a^{1/2}$ for PE-CO₂H (that is, the value of pH at which the surface contains equal numbers of carboxylic acid and carboxylate groups) is ~7.5. Monolayers of fatty acids oriented at the organic/water interface have been reported to have values of $pK_a^{1/2}$ of 7.5.^{52,53} For monolayers at an air/aqueous interface values of $pK_a^{1/2}$ between 7 and 9 have been reported.⁵⁴⁻⁵⁹ The shift in pK_a of carboxylic acids and other indicators in micelles compared to bulk water also agrees with these results.⁶⁰

Salt Effects. As an initial step in rationalizing the form of the curves in Figures 18-21, we have begun an examination of the effect of added salts on the extent of ionization of PE-CO₂H as a function of pH. We have used primarily contact angle methods to obtain these measurements. ATR-IR methods are not easily applicable, because of the difficulty in maintaining a known concentration of a non-volatile salt in the residual liquid film on the surface of the sample during the measurement of the IR spectra. Since these spectra were obtained in systems that exposed the sample to buffers, we suspect that the ionic strength of the liquid in contact with the sample during the spectral measurement was fairly high. Direct potentiometric titration can be used in salt-containing solutions, but is less precise and

convenient than contact angle methods, and has so far proved applicable to UHMW-CO₂H chips and granular PE-CO₂H but not to PE-CO₂H.

Figure 22 presents plots of θ_a vs pH (and, to facilitate internal comparison and comparison with other data, of α_i vs pH) for PE-CO₂H in the presence of added salts. It is evident that certain additives--such as calcium ion--influence the limiting value of θ_a obtained at high pH. Calcium ions form stable, neutral calcium dicarboxylates (which might be less hydrophilic than sodium salts, and thus might raise θ_a at high pH). Lithium ion, by contrast, seems to influence θ_a more at low values of pH than at high values, possibly due to the extreme hydrophilicity of lithium carboxylates. Other ions (sodium, potassium, nitrate) appear to raise θ_a independent of pH, a phenomenon which will be discussed later.

Examination of the values of α_i as a function of pH obtained from these several data shows an unexpected result: that is, the extent of ionization of PE-CO₂H is essentially independent of added salts. Limited data for granular PE-CO₂H (Figure 20) lead to the same conclusion. If the shift and broadening of this curve relative to that for soluble mono- or polybasic acids (Figure 13) were due primarily to Coulombic interactions between carboxylate ions, addition of salts would have been expected to modify this behavior. Certainly added salts decrease ion-ion interactions in polyacrylic acid and other polybasic acids. For example, Figure 23 gives the $pK_a^{1/2}$ (the pH of half ionization) of acetic acid,⁴³ polyacrylic acid,⁴⁴ and PE-CO₂H as a function of the concentration of added sodium chloride. The values for PAA show the shift to lower values of pH with increasing concentration of NaCl expected for a polybasic acid. The values for PE-CO₂H do not. We are, thus, faced with three alternative explanations for the absence of a strong influence of added salts on the extent of ionization of PE-CO₂H: 1) either the origin of the

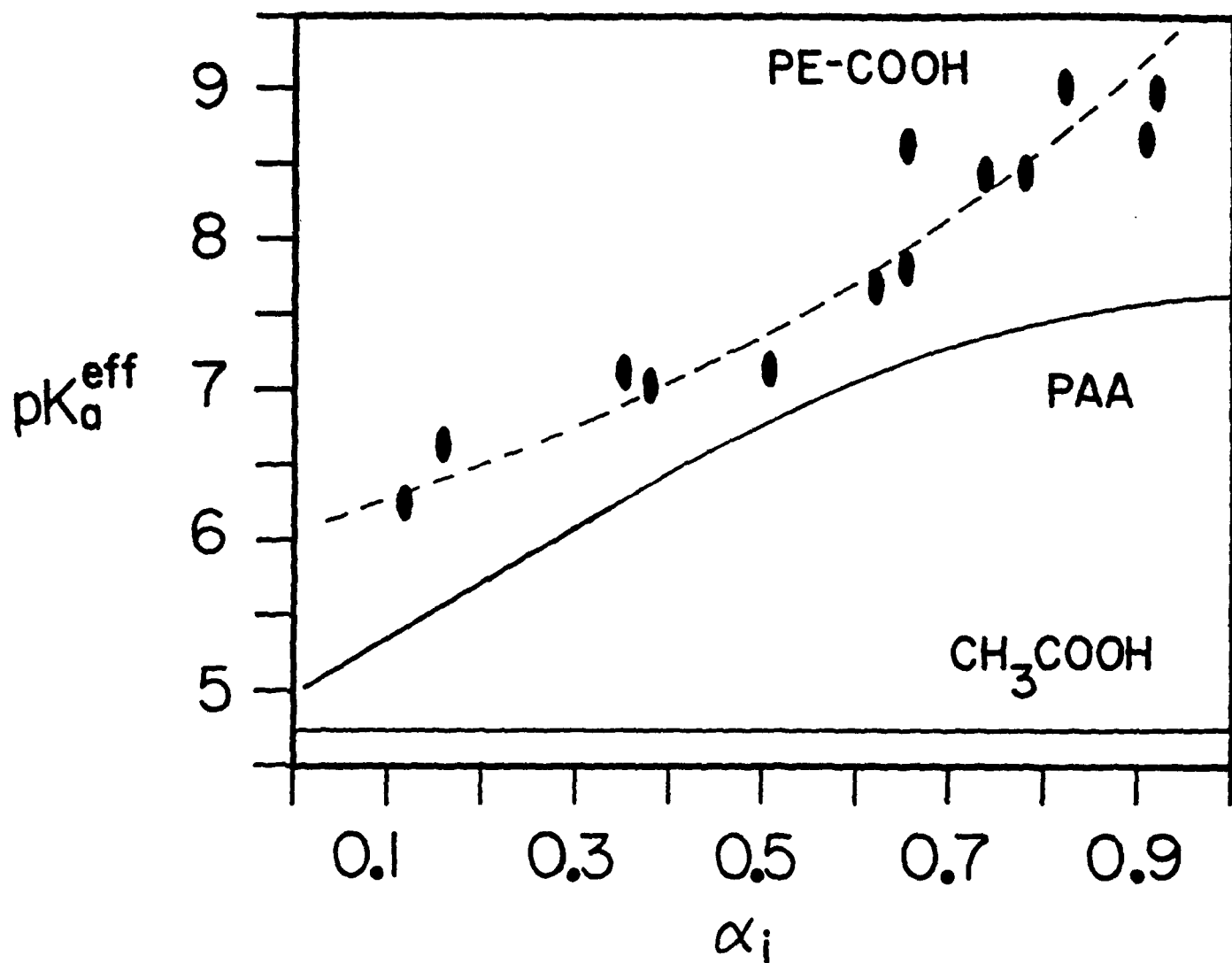


Figure 21. Variation in the effective or apparent pK_a (pK_a^{eff} , eq 11) with the extent of ionization. The dashed line represents a visual fit of eq 10 to data of the sort in Figure 18 shown as \bullet . Curves for poly(acrylic acid) (PAA)⁴⁴ and CH₃CO₂H⁴³ are included for comparison.

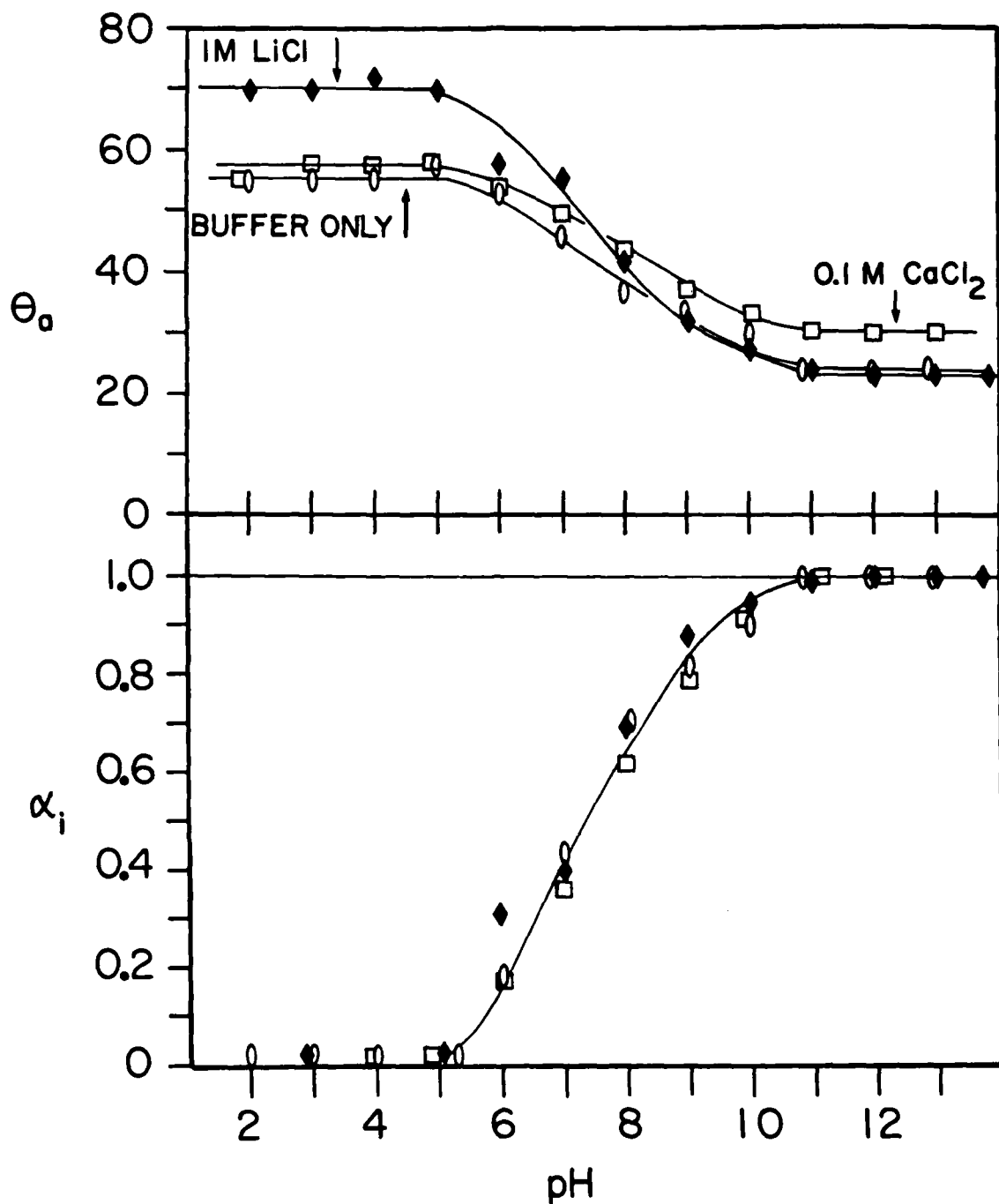


Figure 22. Effects of added salts on θ_a and α_i as functions of pH (all systems were buffered with 0.05 M organic buffers). Salts used: ◆, 1 M LiCl; ○, no added salts; ◻, 0.1 M CaCl₂.

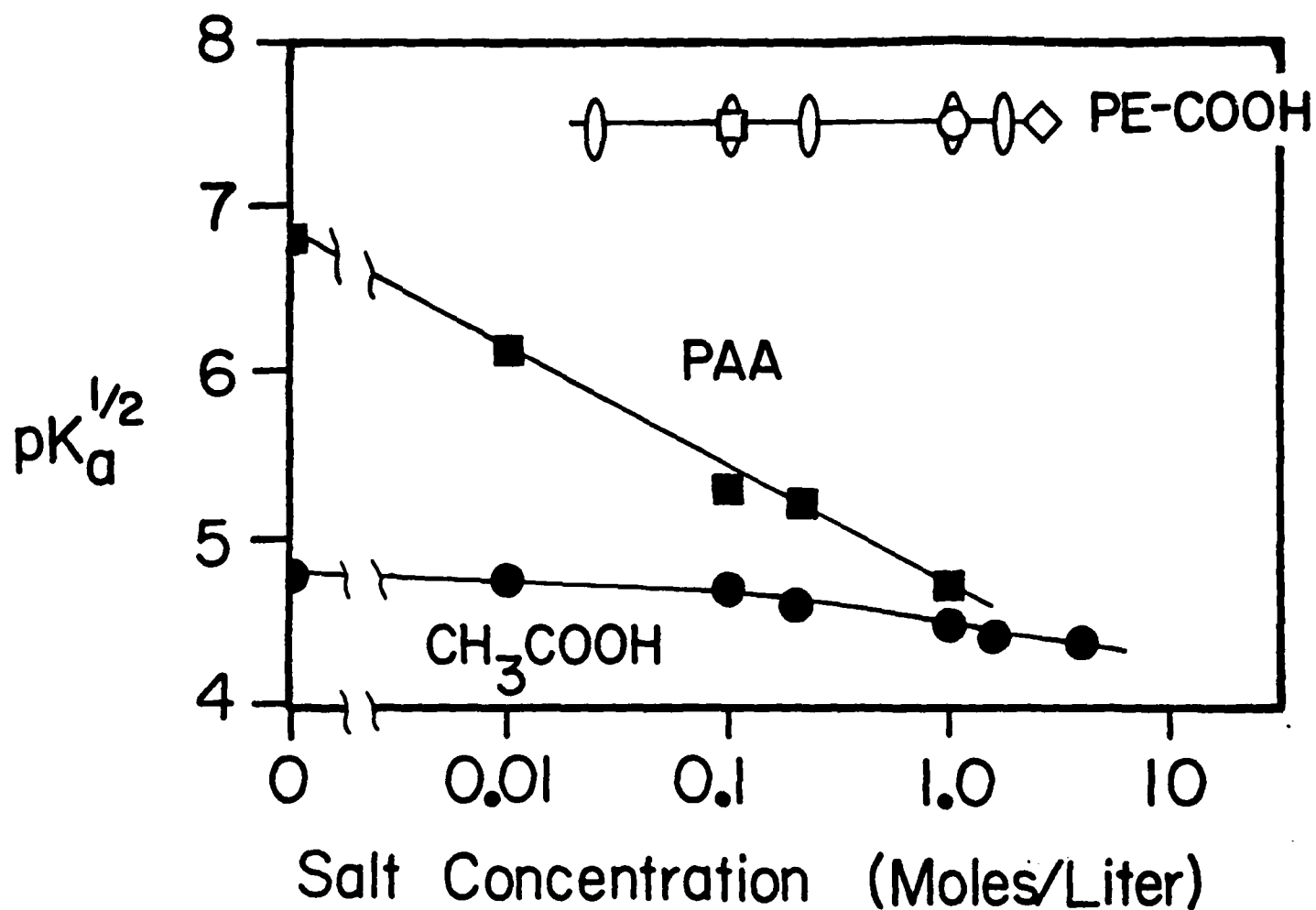


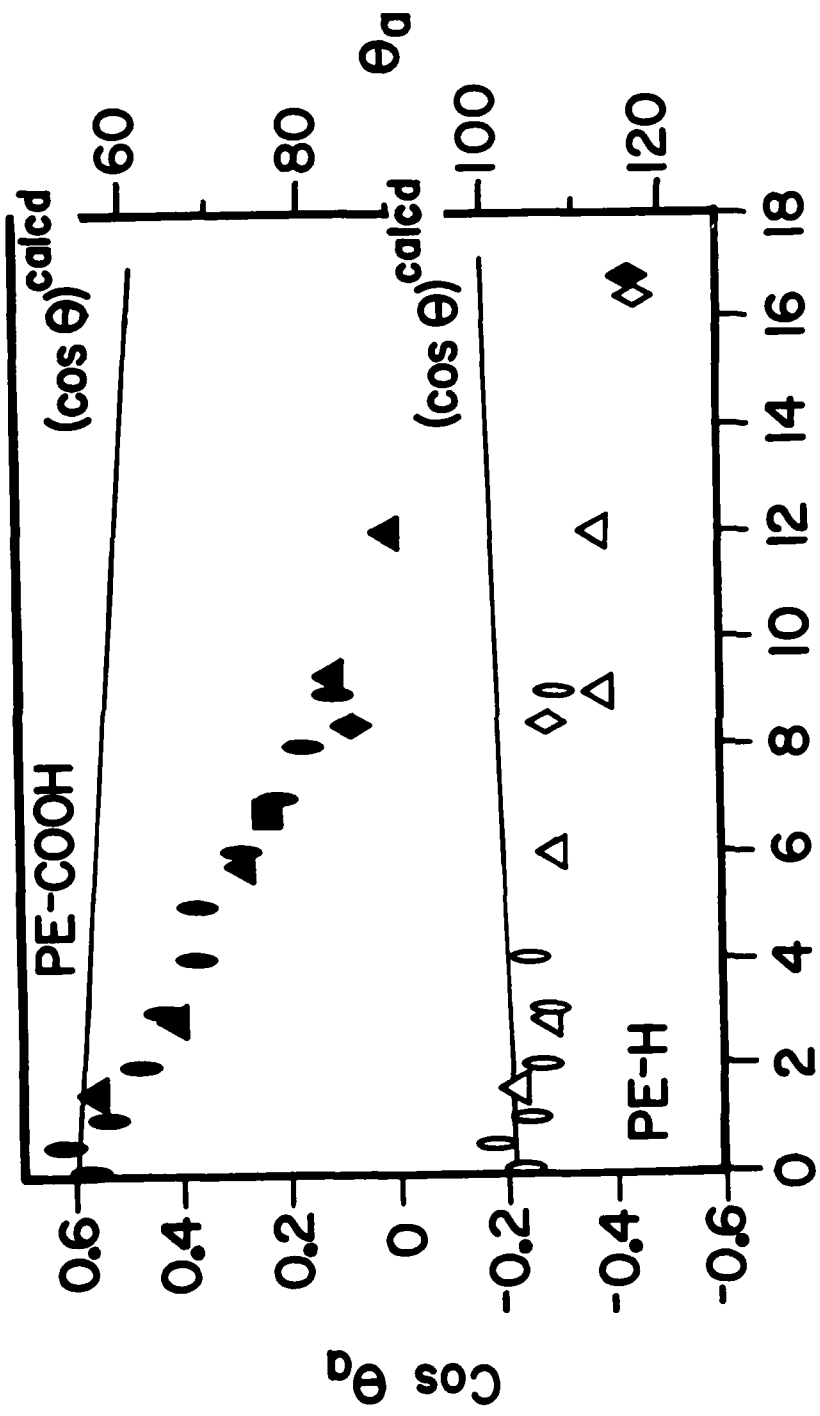
Figure 23. Dependence of the $pK_a^{1/2}$ of PE-CO₂H on aqueous salt concentration: \diamond , NaNO₃; \circ , LiCl; \square , CaCl₂; \bigcirc , NaCl. All solutions also contain 0.05 M buffer. Data for CH₃CO₂H⁴³ and polyacrylic acid (PAA)⁴⁴ in aqueous NaCl are also shown.

deviation from expected monobasic behavior does not lie in ion-ion interactions (or at least in ion-ion interactions which can be influenced by added salts); or 2) salts are unable to approach the carboxylic acids in the interfacial and possibly low dielectric constant region in numbers sufficient to modify the energetics of ion-ion interactions; or 3) the concentrations of buffers present in the contact angle experiments (typically 0.05-0.10 M) have already essentially saturated any salt effect. Unfortunately, our inability to use inverted bubble techniques with PE-CO₂H and the requirement for buffers in sessile drop measurements makes determination of curves of θ vs pH technically impractical at salt concentrations lower than the value of 0.025-0.10 M provided by the buffer. The close similarity of curves for α_i vs pH for UHMW-CO₂H from measurements of contact angles using buffered sessile drops and from direct potentiometric titration in distilled water containing only approximately 1 mM salt (Figure 19) suggest the last explanation is less plausible than the first two.

In the accessible concentration range of added salts ($I = 0.1$ to > 10 M) there is, nonetheless, an influence of ionic strength on θ_a (Figure 22). What is the origin of this influence? Figure 24 summarizes a number of data relevant to this question. This figure plots $\cos \theta_a$ vs ionic strength for PE-CO₂H for a number of salts. According to Young's equation, the relation between $\cos \theta_a$ and surface free energy terms is given by eq (12)

$$\cos \theta_a = \gamma_{LV}^{-1}(\gamma_{SV} - \gamma_{SL}) \quad (12)$$

$$\gamma_{SL} \propto I \quad (13)$$



I (Moles/Liter)

Figure 24. Effect of ionic strength (I) on $\cos \theta_a$ for PE-H and PE-CO₂H.

Salts used: ●, ○, NaClO₄; ▲, △, (NH₄)₂SO₄; ■, ■, NaI; ◆, ◇, AlCl₃.

The changes in $\cos \theta_a$ predicted from changes in γ_{ly} alone (eq 12), using values of γ_{ly} for (NH₄)₂SO₄ as representative are shown for comparison.

Values of γ_{LV} for salt solutions are known.⁷⁰ Taking values for $(\text{NH}_4)_2\text{SO}_4$ as representative, and assuming the term $(\gamma_{SV} - \gamma_{SL})$ to be constant, we calculate the lines labeled $(\cos \theta_a)^{\text{calcd}}$ in Figure 23. The difference between these calculated lines and the observed relation indicates that changes in γ_{LV} are not responsible for the variation in θ_a with ionic strength. It seems improbable that γ_{SV} changes with ionic strength. Thus, it appears that variations in contact angle with ionic strength are due almost entirely to variations in the solid/liquid interfacial free energy and arrive at the experimental result that $\cos \theta_a$ (and thus γ_{SL}) is roughly proportional to the ionic strength of the aqueous solution (eq 13). Although this result is not surprising, we note two important details. First, these effects seem to be non-specific: there is no evidence of trends paralleling the lyotropic series associated with solvation of hydrophobic organic species in aqueous salt solutions.⁷¹ Second, these effects were observed at pH 5, and were therefore obtained on an electrically neutral surface: carboxylic acid groups are not ionized under these conditions.

Conclusions

Oxidation of low-density polyethylene film with chromic acid solution yields a material containing carboxylic acid groups on its surface; the only other important type of polar functional group introduced by this procedure is the carbonyl group (in the form of ketones or aldehydes). The three-dimensional distribution of these groups at the polymer surface is not yet established, but all (> 95%) of them are readily accessible to hydroxide ion, diazomethane, and similar reagents. We infer that these groups are located at or close to the surface of the polymer, in a thin layer. The number of CO_2H groups detected is approximately that expected if the majority of polyethylene

chains at the surface terminate in a CO_2H group. We suggest the structure outlined in Figure 8B as a model for $\text{PE-CO}_2\text{H}$; the most important parameters unspecified by this model are the thickness and structure of the oxidized surface layer.

Titration of the carboxylic acids of oxidized polyethylene with base can be followed in three ways: by ATR-IR, by contact angle, and by direct potentiometric titration. ATR-IR and potentiometric titration appear to sample all of the carboxylic acid groups in the interfacial region: both those on the surface and those in the subsurface region. Contact angle measurements are expected to be specific to surface groups (although the definition of a "surface" group proposed in this paper as one in direct van der Waals contact with the bulk liquid phase remains unsatisfyingly qualitative, and requires additional refinement). Contact angle measurements are experimentally the most convenient of the three, and the only method immediately applicable to both $\text{PE-CO}_2\text{H}$ and $\text{UHMW-CO}_2\text{H}$. We believe, on the basis of this work and experiments to be described in further papers, that studies of wetting--and especially of wetting of surfaces having ionizable functional groups--will provide a particularly sensitive and convenient method for characterizing the physical-organic chemistry of organic surfaces at the microscopic level.

The dependence of the degree of ionization α_i of the carboxylic acid groups of $\text{PE-CO}_2\text{H}$ on the pH of the solution in contact with the surface establishes that this material is not behaving as a simple monobasic acid. The titration curve is broadened and shifted to more basic values of pH than that of monobasic carboxylic acids, or even of polybasic acids such as polyacrylic acid. The relation between α_i and pH does not seem to be an artifact or a function peculiar to $\text{PE-CO}_2\text{H}$: we (in unpublished experiments)

and others⁴⁵⁻⁶¹ have observed similar behavior in systems (Langmuir-Blodgett films, colloids, micelles) having quasi-two dimensional arrays of functional groups. The detailed rationalization of the form of the relationship between α_i and pH has not yet been defined for any of these systems, nor has it been established that the apparently similar forms shared by them have a common origin.

We and others have suggested three possible (and not necessarily independent) explanations for the type of acid-base behavior displayed by PE-CO₂H; these explanations are summarized schematically in Figure 25. The first is that the characteristics of this system are determined primarily by Coulomb interactions between carboxylate ions (Figure 25A). The second explanation is that dipolar effects at the interface play an important role in determining the behavior of PE-CO₂H (Figure 25B).⁵⁷ Both carboxylic acid and carboxylate groups have large dipole moments. Thus, there should exist a high electrostatic field gradient at the polymer-water interface. This high field gradient might alter the local pH or change the dielectric response of the water at the interface, both of which would be expected to influence the acid-base behavior of a carboxylic acid group located at the interface.^{57,60,62,66} A third type of influence on the behavior of carboxylic acid groups at the polymer-water interface could arise from a local dielectric cavity effect (Figure 25C): the carboxylic acid is required to ionize in a medium composed of polyethylene and water. One might expect that it would be more difficult to place a negative charge at or in an interface of this type than to form one in homogeneous solution in which solvation is less hindered.^{57,60,66}

It is not yet clear which of these effects is most important, but the unexpectedly small influence of the ionic strength of the medium on the extent

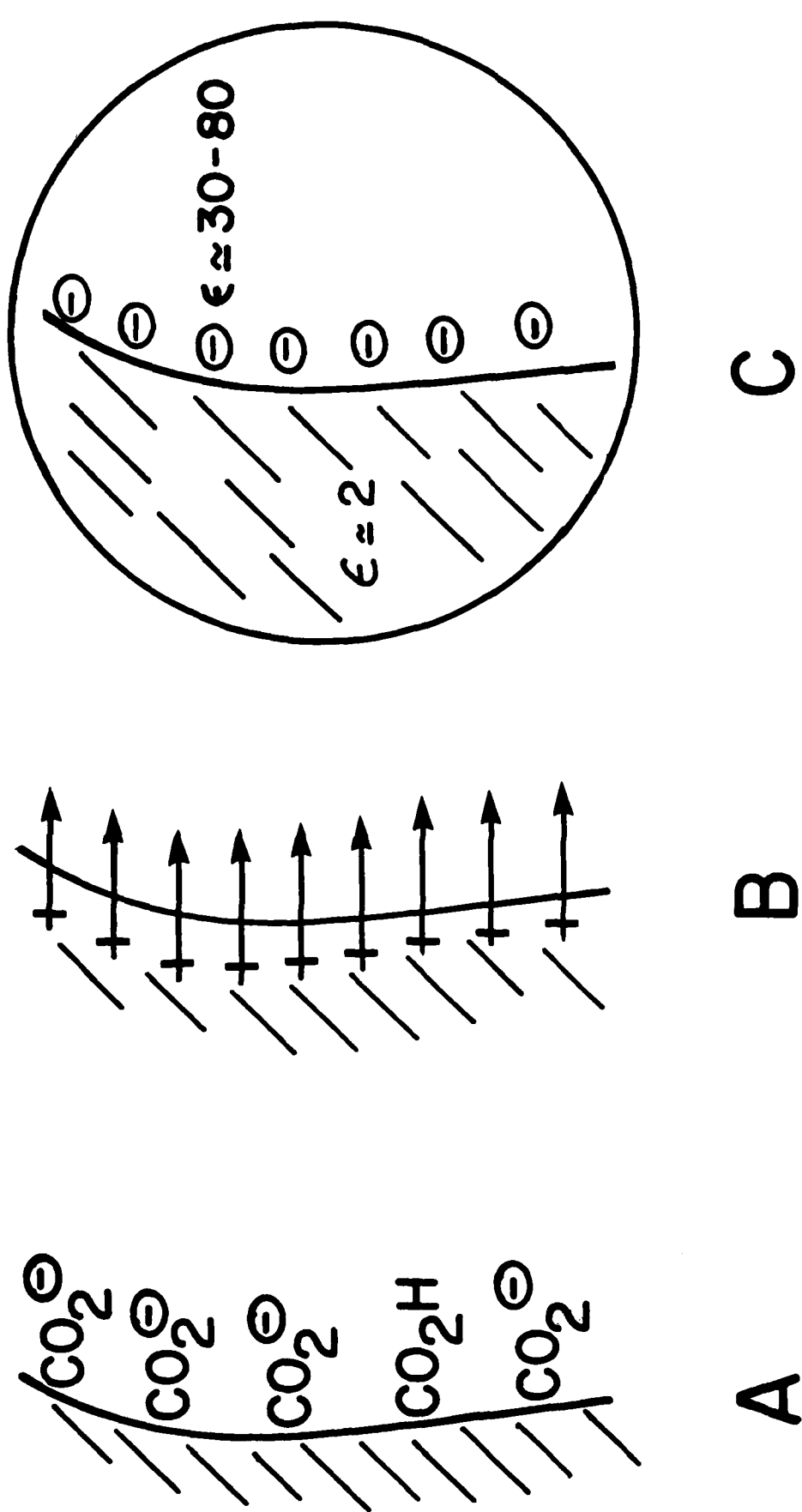


Figure 25. Schematic diagrams illustrating three possible factors influencing the ionization of surface-bound carboxylic acids. These are: A, ion-ion interactions; B, dipolar interactions between the functional groups on the surface and the solvent; C, the low "average" dielectric constant of the PE-CO₂H/H₂O interface.

of ionization of PE-CO₂H suggests that a model involving simple Coulomb interactions within a homogeneous population of carboxylic acid groups may not be adequate to rationalize the wetting behavior of this material. Since some fraction of the carboxylic acid groups (perhaps the majority) are located in the subsurface region--in proton-transfer equilibrium with the liquid medium but removed from the region that determines contact angle--it is plausible that the carboxylic acid moieties may represent a heterogeneous population with different values of pK_a , and that this heterogeneity may influence the shape of the relation between α_i and pH. The fact that contact angle and ATR-IR suggest similar values of α_i at a given pH suggests that surface groups (sensed by contact angle) and subsurface groups (sensed by ATR-IR) behave similarly. Heterogeneity may also exist along the surface (for example, on crystalline and amorphous regions). We are continuing to explore this problem experimentally.

Although we are not yet able to rationalize the acid-base behavior of PE-CO₂H theoretically, our present results have three immediately useful consequences. First, the good general agreement between titrations followed by ATR-IR, contact angle, and potentiometry provide support for the reliability of the convenient and versatile contact angle methods, and offer empirical justification for the assumptions underlying the development of eq 6. Second, these results establish the experimental conditions required for the interconversion of PE-CO₂H and PE-CO₂⁻. The ability to modify significantly the wetting behavior of a representative polymer surface without changing surface morphology should prove useful in studies of adhesion, corrosion, tribology, and related complex materials problems. Third, the difference between contact angle data obtained using buffered and unbuffered solutions should also be useful in certain types of surface analyses: in

particular, measurement of contact angle using small liquid drops and surfaces containing high concentrations of ionizable surface groups offers a convenient, semi-quantitative method for counting surface functionality and for following the course of certain types of derivatizing reactions.

Acknowledgment. Electron microscopy was carried out using instruments in the Harvard Materials Research Laboratory. Our colleagues Barry Troughton, Yu Tai Tao, Lou Strong, Colin Bain, Joe Evall, and Stephen Wasserman have provided information concerning model systems essential to the interpretation of the work reported here. We thank Drs. Ralph Nuzzo (Bell Laboratories) and Dave Allara (Bell Communications Research) for essential discussions concerning surface chemistry.

Experimental Section

General. Dichloromethane and methanol were Mallinckrodt nanograde; dimethylsulfoxide was MCB reagent grade; THF and acetone and all other solvents were reagent grade; all were used as received. Doubly-distilled water was redistilled in a Corning model AG-1b glass distillation apparatus. N-nitrosomethylurea (Pfaltz and Bauer), 1-ethyl-3-(3-dimethylaminopropyl)carbodiimide hydrochloride (Sigma) and glycine ($2\text{-}^3\text{H}$) (New England Nuclear as a 15.0 Ci/mmol sample in 0.1 N HCl) were used as obtained. Scanning electron micrographs were obtained on a JEOL 35 U microscope at 0° tilt and 20 kV after sputter coating the samples with $\sim 200 \text{ \AA}$ of gold/palladium (5% Pd) using a Hummer II (Technics) at 10 mA, 2,500 V and 0.5 torr of argon for 20 sec. ESCA spectra were obtained on a Physical Electronics Model 548 spectrometer (MgK α X-ray source, 100 eV pass energy, 10^{-8} to 10^{-9} torr, machine calibrated according to ASTM STP 699). Spectra were obtained either in survey mode for quick comparisons or by collecting data only at desired regions of binding energy for more accurate quantification using the software supplied by Perkin Elmer.

Potentiometric Titrations. The direct potentiometric titrations were performed using a Chemitrix type 40E pH meter and an Aldrich minielectrode #Z11336-0. The samples were made by suspending the granular PE-CO $_2$ H (or UHMW-CO $_2$ H chips) in 15 mL of doubly distilled water. To this suspension was added 100 μL of 0.100 N HCl (Harleco). The pH values of the samples were monitored as 0.100 N NaOH (Ricca) was added in 20- μL portions (using a Gilson 100- μL Pipetman) with vigorous magnetic stirring under N $_2$. The difference in the quantity of base required for each suspension and the control containing only water represents the buffering capacity of the PE-CO $_2$ H in that sample (granular PE-CO $_2$ H or UHMW-CO $_2$ H chips).

ATR-IR Measurements. Films were cut to the size of the KRS-5 (thallium bromide/iodide, 45°) crystal faces and pressed against the faces with an MIR (Perkin Elmer) sample holder. Films treated with aqueous solution prior to ATR-IR spectra determination (such as PE-CO₂⁻Na⁺) were blotted dry on filter paper and dried in vacuum (60 min, 0.01 torr, room temp) prior to contact with the KRS-5 crystal to prevent crystal damage and to eliminate excess water peaks from the spectrum. Rectangular pieces of thin cardboard the same size as the films were inserted between the films and the steel sample holder to distribute the pressure on the film evenly. Transmission spectra were obtained on a Perkin Elmer Model 598 spectrometer and converted directly to absorption spectra, by computer, for quantification. To account for differences in absorption due to slightly different degrees of contact between the polyethylene sample and the KRS-5 reflection element the absorbance peaks were always quantified relative to other peaks in the spectrum. In determining the ionization of the carboxylic acids at a given pH, for example, only the relative integrated absorbances at 1560 cm⁻¹ (CO₂⁻) and 1710 cm⁻¹ (CO₂H) were considered.

Contact Angle Measurements. Contact angles were determined on a Ramé-Hart Model 100 contact angle goniometer equipped with an environmental chamber by estimating the tangent normal to the drop at the intersection between the sessile drop and the surface. These were determined 5-20 seconds after application of the drop. The humidity in the chamber was maintained at 100% by filling the wells in the sample chamber with distilled water. The temperature was not controlled and varied between 20 and 25 °C. The volume of the drop used was always 1 μL. Polyethylene samples were cut to a size of 0.5 x 2 cm and attached by the back of the sample to a glass slide using two-sided Scotch tape to keep the sample flat. All reported values are the

average of at least eight measurements taken at different locations on the film surface and have a maximum error of $\pm 3^\circ$.

Polyethylene (PE-H). Low density biaxially blown polyethylene film (100 μm thick) was a gift from Flex-O-Glass Inc. (Flex-O-Film DRT-600B). The film was cut into 10 x 10 cm squares. These were extracted by suspending the film in refluxing CH_2Cl_2 for 24 h to remove antioxidants and other film additives. The removal of additives can be monitored using the carbonyl region of the ATR-IR spectrum. Prior to extraction a peak at 1650 cm^{-1} is present. This peak is eliminated by the extraction. Some samples were thermally annealed in a vacuum (100 $^\circ\text{C}$, 0.01 torr, 4 days) to increase the high temperature stability of the surface. Samples treated in this manner gave results indistinguishable from those described for unannealed film in all experiments reported. All samples were dried under vacuum (20 $^\circ\text{C}$, 0.01 torr, 4 h) prior to oxidation to remove any residual solvent. Those samples not to be oxidized were stored under dry argon. Monsanto K-2400-212 polyethylene film was also used in several experiments. In all cases, experiments were performed on the side of film facing the inside of the stock roll.

Polyethylene Carboxylic Acid (PE-CO₂H). PE-H was oxidized by floating on $\text{H}_2\text{SO}_4/\text{H}_2\text{O}/\text{CrO}_3$ (29/42/29; w/w/w) at 72 $^\circ\text{C}$ for 60 sec (or other time if indicated). The samples were rinsed four times in doubly distilled water, once in acetone, dried in air for 1 h and stored under dry argon. The samples had a peak in the ATR at 1710 cm^{-1} .

Granular PE-CO₂H and Derivatives. Granular polyethylene (U.S. Industrial Chemicals Corp., 5 g, $\sim 0.3\text{ mm}$ chunks, $\rho \approx 0.91$) was oxidized by suspending in chromic acid solution ($\sim 60\text{ mL}$) at 72 $^\circ\text{C}$ for 5 min. The surface-oxidized polymer grains were rinsed in water five times, methanol twice, and dried in air. The methyl ester, granular PE-CO₂CH₃, was made by stirring granular

PE-CO₂H in 75 mL of methanol containing 15 mL of sulfuric acid at 40 °C for 18 h. The grains were rinsed 3 times in methanol, once in water, once again in methanol and dried in air. This material was hydrolyzed in 25% KOH for 10 min at 40 °C, rinsed 5 times in water, and once in methanol to reform granular PE-CO₂H.

UHMW-CO₂H. Ultra high molecular weight polyethylene sheet (AIN Plastics, Inc., Mt. Vernon, NY, 1/8" thick, $\rho \approx 0.93$) was cut with a handsaw. The resulting ejected chips (7 g, ≈ 0.1 -1.0 mm chunks) were collected and oxidized by suspending in chromic acid solution at 72 °C for 5 min. The chips were rinsed in water 5 times and methanol once. These chips were used for the direct potentiometric titrations. Alternatively the surface of the sheet itself (5 cm²) was oxidized by floating on chromic acid solution for 5 min (or other time if indicated). This material was rinsed in water 5 times, methanol once, and dried in air. The oxidized surface of the sheet was used for measurements of θ_a .

Treatment of PE-CO₂H with NaBH₄ to Remove Ketone and Aldehyde Functions. A solution of 4 g of NaBH₄ (98%, Alfa) in 100 mL of 0.1 M NaOH was heated to 50 °C. PE-COOH was added and stirred for 2 h, removed, and immersed in 1 N HCl for 10 min. The film was rinsed in water, 1 N HCl, three times in doubly distilled water, and once each in methanol and methylene chloride. The ESCA spectrum was indistinguishable from PE-COOH. The water contact angle was 54° and the sample had a new ATR-IR peak at 3350 cm⁻¹.

PE-CH₂OH. PE-COOH was treated with excess 1 M BH₃·THF (Aldrich) at 50 °C for 20 h under argon. The films were rinsed twice with water, soaked in 1 N HCl for 5 min and rinsed 3 times with water. The carbonyl ATR-IR peaks were absent and a new peak (3350 cm⁻¹) appeared.

$\text{PE-CH}_2\text{OCOCF}_3$. PE-CH₂OH was allowed to react with 3 mL of trifluoroacetic anhydride (Aldrich) in 28 mL of dry diethyl ether. The mixture was refluxed for 3 h and the films rinsed 5 times with diethyl ether, 5 times with acetone and 3 more times with ether. The ATR-IR spectra showed new peaks at 1790 cm⁻¹ (CF₃CO₂R), 1165 cm⁻¹ and 1225 cm⁻¹ (C - F).

PE-COCl . PE-COOH was soaked in 30 mL of dry ether containing 3 g of PCl₅ for 1 h at rt. The film was quickly removed and used immediately without workup to minimize hydrolysis of the acid chloride groups by ambient water vapor.

$\text{PE-CO}_2\text{CH}_3$. Methyl esters were made by three different methods.

a) PE-CO₂H was soaked in anhydrous ether (30 mL) containing 3 g of PCl₅. After 1 h the film was removed and immediately immersed in 100 mL of anhydrous methanol. After stirring (being careful to prevent the magnetic stirring bar from hitting the film) for 30 min the film was washed three times with doubly distilled water and once with acetone. b) Diazomethane was generated by adding 2 g of N-nitrosomethylurea to a mixture containing 20 mL of diethyl ether and 6 mL of 40% w:w potassium hydroxide in water at 0 °C.⁷² The mixture was stirred at 0 °C for 30 min and the yellow ether portion was decanted into a test tube containing PE-CO₂H. After reacting for 5 min the film was removed, washed three times with doubly distilled water and once with acetone. c) PE-CO₂H was stirred for 18 h in 500 mL of anhydrous methanol containing 75 mL of H₂SO₄ at 40 °C. The film was rinsed twice with methanol, three times with doubly distilled water and once with acetone. For all three methods ATR-IR spectra showed a new peak at 1740 cm⁻¹ and no CO₂⁻ peak (1560 cm⁻¹) after treatment with 1 N NaOH, indicating complete reaction.

$\text{PE-CO}_2\text{R}$. The ethyl, bromoethyl, propyl and octyl esters were made by soaking PE-CO₂H in the appropriate anhydrous alcohol (50 mL) containing

sulfuric acid (10 mL) at 40 °C for 18 h. The films were worked up as for PE-CO₂CH₃. Alternatively the propyl ester was made by putting PE-COCl in propan-1-ol for 30 min and rinsing with CH₃OH, water (twice) and acetone.

PE-CONHNH₂. PE-CO₂CH₃ (made in CH₃OH/H₂SO₄) was heated to 50 °C in 95% NH₂NH₂ (Eastman) for 1 h. The film was rinsed 3 times in methanol and twice in water. The ATR-IR spectrum shows a new peak at 1650 cm⁻¹.

PE-CONCHCH₂CO₂H: Radioactive Labeling, Release, and Counting. The fluorescence assay using 4-methyl-7-hydroxycoumarin has been reported.⁵ Surface sites were also determined by tritium labeling. PE-CO₂H (1 cm x 1 cm) was submersed in 30 mL of dimethylsulfoxide containing 0.5 g of N-hydroxysuccinimide and 0.5 g of 1-ethyl-3-(3-dimethylaminopropyl)carbodiimide hydrochloride for 12 hours to produce PE-CO-N-hydroxysuccinimide (PE-CONHS). The PE-CONHS was washed with dimethylsulfoxide, then with dichloromethane, and allowed to react with a solution of tritiated glycine for 1 h. The tritiated glycine solution was prepared by adding 4.0 mg of nonlabeled glycine to 800 μL of 1 mCi/L (15.0 Ci/mole) tritiated glycine and 200 μL of water, then adjusting the pH of the solution to ca 10 with Na₂CO₃. The films were removed, washed six times with 100-mL portions of water and allowed to dry on filter paper. The dry films were sealed into glass ampoules containing 0.5 mL of 6 N HCl and heated at 110 °C for 12 h. After cooling the samples, the liquid was transferred to scintillation vials containing 15 mL of scintillation fluid. Radioactive samples were counted in New England Nuclear Aquasol scintillation fluid on a Beckman LS 100C liquid scintillation counter. The solutions gave 85,000-90,000 dpm (16 x 10¹⁴ sites/cm²). Films after hydrolysis, measured directly, had <3% of the activity prior to hydrolysis. Unoxidized polyethylene treated in the same manner had <1% of the activity of oxidized polyethylene.

Notes and References

1. This work was supported in part by the Office of Naval Research.
Correspondence should be addressed to GMW at Harvard University.
2. IBM Predoctoral Fellow in Polymer Chemistry, 1984-86.
3. NCI Predoctoral Trainee, 1980-81.
4. National Science Foundation Predoctoral Fellow, 1978-81.
5. Rasmussen, J. R.; Stedronsky, E. R.; Whitesides, G. M. J. Am. Chem. Soc. 1977, 99, 4736.
6. Rasmussen, J. R.; Bergbreiter, D. E.; Whitesides, G. M. J. Am. Chem. Soc. 1977, 99, 4746.
7. Blais, P.; Carlsson, J.; Csullog, G. W.; Wiles, D. M. J. Coll. Int. Sci. 1974, 47, 636.
8. Kato, K. J. App. Polym. Sci. 1977, 21, 2735.
9. Bassett, D. C. "Principles of Polymer Morphology"; Cambridge University Press: Cambridge, 1981.
10. Olley, R. H.; Hodge, A. M.; Bassett, D. C. J. Polym. Sci.: Polym. Phys. Ed. 1979, 17, 627.
11. Baszkin, A.; Ter Minassian-Saraga, L. Polymer 1978, 19, 1083.
12. Clark, D. T.; Feast, W. J. "Polymer Surfaces"; Wiley-Interscience: New York, 1978.
13. Brewis, D. M. J. Material Sci. 1968, 3, 262.
14. Briggs, D.; Zichy, V. J. I.; Brewis, D. M.; Comyn, J.; Dahm, R. H.; Green, M. A.; Kinieczko, M. B. Surface Interface Anal. 1980, 2, 107.
15. Eriksson, J. C.; Golander, C.-G.; Baszkin, A.; Ter-Minassian-Saraga, L. J. Coll. Int. Sci. 1984, 100, 381.
16. Adamson, A. W. "Physical Chemistry of Surfaces"; Wiley: New York, 1982.

17. Vold, R. D.; Vold, M. J. "Colloid and Interface Chemistry"; Addison-Wesley: Reading, MA, 1983. Jaycock, M. J.; Parfitt, G. D. "Chemistry of Interfaces"; John Wiley and Sons: New York, 1981.
18. Good, R. J.; Stromberg, R. R. "Surface and Colloid Science"; Plenum: New York, 1979; Vol. II.
19. Joanny, J. F.; de Gennes, P. G. J. Chem. Phys. 1984, 81, 552.
20. Kaelble, D. H. "Physical chemistry of Adhesion"; Wiley: New York, 1971; p 170.
21. Gould, R. F., Ed. Advan. Chem. Ser., 1964 43.
22. Schwartz, L. W.; Garoff, S. Langmuir 1985, 1, 219.
23. Cherry, B. W. "Polymer Surfaces"; Cambridge University Press: Cambridge, 1981.
24. Woodruff, D. P. "The Solid-Ligand Interface"; Cambridge University Press: Cambridge, 1981.
25. Fortes, M. A. J. Chem. Soc., Faraday Trans. 1 1982, 78, 101.
26. Malev, V. V.; Gribanova, E. V. Dokl. Akad. Navk. SSSR 1983, 272, 413.
27. Faust, R.; Wolfram, E. Anales Universitatie Scientiarum Budapest 1980, 151.
28. Baszkin, A.; Ter-Minassian-Saraga, L. J. Coll. Int. Sci. 1973, 43, 190.
29. Ionization of CO₂H groups outside of the drop due to diffusion of acid or base along (or in) the surface can possibly change γ_{SV} . This possibility is addressed in an upcoming paper.
30. Young, T. In "Miscellaneous Works"; Peacock, G., Ed.; Murray: London, 1855; Vol. 1, p 418.
31. Our estimate of the value of β_{CO_2H} is based on studies of self-assembled Langmuir-Blodgett-like monolayers. Using systems composed of organic thiols of structure HS(CH₂)₁₀₋₂₀CO₂H adsorbed on evaporated gold films,

we can prepare surfaces having essentially monolayer coverage of CO_2H groups. Water spreads on these surfaces [$\theta_a(\text{pH } 3) \sim 0^\circ$] [B. Troughton, unpublished]. Making the four assumptions that this value of θ_a characterizes a surface with $\beta_{\text{CO}_2\text{H}} = 1$, that the value observed for polyethylene ($\theta_a = 103^\circ$) is that characterizing a surface with $\beta_{\text{CH}_2} = 1$, that equations 1 and 2 are valid, and that the surface of $\text{PE-CO}_2\text{H}$ exposes only CO_2H and CH_2 groups to the drop of water, we estimate from the observed value of $\theta_a(\text{pH } 3) = 55^\circ$ that $\beta_{\text{CO}_2\text{H}} \approx 0.65$. Inclusion of ketone or aldehyde groups into the population of polar functionality on the surface of $\text{PE-CO}_2\text{H}$ would lower this estimate of $\beta_{\text{CO}_2\text{H}}$. Further, it is possible that $\theta_a = 0$ for surfaces with values of $\beta_{\text{CO}_2\text{H}} < 1$, although we do not yet know what value of $\beta_{\text{CO}_2\text{H}}$ is necessary to just cause θ_a to reach 0° . This possibility suggests that even in the absence of ketones or aldehydes the estimated value of $\beta_{\text{CO}_2\text{H}}$ must be an upper limit.

32. S. R. Holmes-Farley, to be published.
33. Alexander, A. E.; Hibberd, G. E. In "Techniques of Chemistry," Vol. I (V); Weissberger, A.; Rossiter, B. W., Eds.; Wiley-Interscience: New York, 1972; p 575.
34. Mack, G. L. J. Phys. Chem. 1936, 40, 159.
35. There appear to be two plausible explanations for the resistance of the surface of $\text{PE-CO}_2\text{H}$ to contamination. First, the surface may simply not attract contaminants from the air as rapidly as a surface with a higher value of the interfacial free energy, γ_{SV} , such as gold. Second, contaminants which adsorb onto the surface of polyethylene may be able to dissolve into the bulk polymer beneath the surface and leave the surface relatively clean. A similar phenomenon would not be possible with metals, and improbable with inorganic materials.

36. This estimate is based on the relative absorbances of carboxylic acids and ketones, $\epsilon_{\text{ketone}}/\epsilon_{\text{acid}} = 2.4$, in polyethylene [Rugg, F. M.; Smith, J. J.; Bacon, R. C. J. Polym. Sci. 1954, 13, 535]. This ratio is also supported by completely independent experiments involving ESCA spectroscopy. The atomic surface composition of PE-CO₂H (determined as in Figure 7) after converting the carboxylic acid groups to amide groups (PE-CONH₂) made by reacting PE-COCl with ammonium hydroxide and rinsing with water) was 39.7% C, 6.5% O and 3.8% N. This N/O ratio of 0.58 is also the ratio of amides to ketones plus amides. Thus carboxylic acid groups comprise ~60% of the surface carbonyl functionality. (PE-H treated in the same manner showed no ESCA signal attributable to nitrogen).
37. The surface concentrations were determined by integrating the area under the peaks and were corrected by dividing by the area sensitivity factors for the different elements supplied with the Perkin Elmer software package used to integrate the peaks. The area sensitivity factors were: C_{1s}, 0.25; O_{1s}, 0.67; N_{1s}, 0.43; S_{2p}, 0.53; Br_{2p}, 2.3.
38. We have previously obtained $20 \times 10^{14} \text{ cm}^{-2}$ for a more heavily oxidized surface (5 min oxidation instead of 1 min) using derivatives of 7-hydroxycoumarin covalently attached to the surface (ref 5).
39. This surface actually contains both primary and secondary hydroxyl groups derived from carboxylic acid and ketone groups respectively.
40. Other ionizable groups such as amines do show such breaks. Studies of these groups are the subject of another paper.
41. It is possible that some of the surface functional groups lie below the region sensed by contact angle measurements (a few Å) and that the conversion of such groups remains undetected. This possibility is dealt

with in an upcoming paper concerning derivatization of the polyethylene surface.

42. Fieser, L. F.; Fieser, M. "Reagents for Organic Synthesis"; Wiley: New York, 1967; Vol. I, p 1049.
43. Lumme, P. O. Suomen Kemistilehti 1956, B29, 217.
44. Gregor, H. P.; Frederick, M. J. J. Polym. Sci. 1957, 23, 454-465.
45. Buffers are: HEPES, N-2-Hydroxyethylpiperazine-N'-2-ethanesulfonic acid; CHES, 2-(N-Cyclohexylamino)ethanesulfonic acid; MOPS, 3-(N-Morpholino)-propanesulfonic acid; TAPS, tris(Hydroxymethyl)methylaminopropanesulfonic acid; TRIS, tris(Hydroxymethyl)aminomethane; phosphate; and triethanolamine.
46. The distinction between "advancing" and "stationary" contact angles is not an entirely clear one. The drops here were allowed to stop their spontaneous advance, but were not vibrated or otherwise manipulated (cf ref 18 p 38).
47. We have also attempted to overcome this problem by using inverted bubble techniques in which the volume of solution in contact with the surface of the polymer is large. Inverted bubble techniques are, however, effectively procedures which measure the receding contact angle θ_r . Since $\theta_r \leq 5^\circ$ for PE-CO₂H this technique is not useful for this material.
48. The buffers used were the same as those listed in footnote 45, with the exception that CHES was not used.
49. Tokiwa, F.; Ohki, K. J. Phys. Chem. 1967, 71, 1824.
50. Yalkowsky, S. H.; Zografis, G. J. Coll. Int. Sci. 1970, 34, 525.
51. Katchalsky, J. M.; Spitnik, P. J. Polym. Sci. 1957, 23, 513.
52. Peters, R. A. Proc. Roy. Soc. A. 1931, 133, 140.
53. Danielli, J. F. Proc. Roy. Soc. B 1937, 122, 155.

54. Shulman, J. H.; Hughes, A. H. Proc. Roy. Soc. A 1932, 138, 430.
55. Glazer, J.; Dogan, M. Z. Trans. Faraday Soc. 1953, 49, 448.
56. Sanders, J. V.; Spink, J. A. Nature (London) 1955, 175, 644.
57. Betts, J. J.; Pethica, B. A. Trans. Faraday Soc. 1956, 52, 1581.
58. Davies, J. T.; Rideal, E. K. "Interfacial Phenomena"; Academic Press, 1963; pp 237-238.
59. Bagg, J.; Haber, M. D.; Gregor, H. P. J. Coll. Int. Sci. 1966, 22, 138-143.
60. Fernandez, M. S.; Fromherz, P. J. Phys. Chem. 1977, 81, 1755.
61. Tokiwa, F.; Ohki, K. J. Phys. Chem. 1967, 71, 1824.
62. Mille, M. J. Coll. Int. Sci. 1981, 81, 169.
63. Lifson, S.; Kaufman, B.; Lifson, H. J. Chem. Phys. 1957, 27, 1356.
64. Laskowski, M.; Scheraga, H. A. J. Am. Chem. Soc. 1954, 76, 6305.
65. Mille, M.; Van der Kooi, G. J. Coll. Int. Sci. 1977, 61, 475.
66. Lukac, S. J. Phys. Chem. 1983, 87, 5045.
67. Caspers, J.; Goormaghtigh, E.; Ferreira, J.; Brasseur, R.; Vandenbranden, M.; Ruyschaert, J. M. J. Coll. Int. Sci. 1983, 91, 546.
68. Lifson, S.; Kaufman, B.; Lifson, H. J. Chem. Phys. 1957, 27, 1356.
69. We are attempting to distinguish between these hypotheses both theoretically and using highly ordered, oriented monolayer films.
70. Herz, W.; Knaebel, E. Z. Phys. Chem. 1931, 31, 389.
71. For example, Robinson and Jencks (Robinson, D. R.; Jencks, W. P. J. Am. Chem. Soc. 1965, 87, 2470) report that $(\text{NH}_4)_2\text{SO}_4$ strongly "salts out" acetyltetraglycine ethyl ester while NaClO_4 has a strong "salting-in" effect. Although the origin of this "salting-out" effect is still a subject of debate, in one interpretation it is considered to reflect the effect of ions on the interfacial tension between the solute and the

water (Bull, H. B.; Breese, K. Arch. Biochem. Biophys. 1980, 202, 116).

For general references see: Arakowa, T.; Timasheff, S. N. Biochemistry 1982, 21, 6536, 6545. Tanford, C. "The Hydrophobic Effect"; Wiley-Interscience: New York, 1973.

72. Blatt, A. H. "Organic Syntheses Collective"; Wiley: New York, 1943; Vol. II, pp 165-167.

Captions

- Figure 1. Dependence of advancing contact angle (θ_a) of buffered (●) and unbuffered (○) aqueous solutions on PE-COOH. Unoxidized polyethylene (PE-H) is shown as a control. The buffer used was 0.10 M phosphate.
- Figure 2. Schematic representations of an ideal (A) and real (B) drop of liquid (L) in contact with solid (S) and vapor (V) with contact angle θ . The symbols in B represent: ○, water molecules; △, dissolved solutes (phosphate, buffer salts); ◆, ◆, polar surface groups (CO₂H, CO₂⁻, C=O,...); ■, nonpolar surface groups (CH₂, CH₃,...).
- Figure 3. Surface area (idealized planar area, mm²) and effective concentration of surface groups (mM) under a 1-μL drop, for various values of θ_a , calculated using eq 7. The construction used to arrive at eq 7 is shown at the top of the figure. The shape of the drop is assumed to be a portion of a sphere of radius r . The density of CO₂H groups is assumed to be $20 \times 10^{14} \text{ cm}^{-2}$ (that is, the measured density on PE-CO₂H; for a planar close-packed monolayer, the values of effective molarity given in the figure should be divided by $\sqrt{4}$).

Figure 4. Advancing contact angle for water at pH=3 (HCl, open symbols) and pH=13 (NaOH, filled symbols) for samples of low density polyethylene film (PE) and ultra high molecular weight polyethylene sheet (UHMW) oxidized for times indicated, using the standard procedure (see Text): ○, ●, unannealed; □, ■ annealed 100 °C for 96 h; ◇, ◆ annealed 110.6 °C, 24 h; ▲, △ unannealed Monsanto K-2400-212 polyethylene. Extended oxidation of either material increases the roughness of the surface, but does not change the contact angle at pH 3 or pH 13.

Figure 5. Variation of contact angle (using water at pH 5 and pH 12) of PE-CO₂H with time of storage under different conditions. Films were not previously annealed; T = 20 °C. Storage conditions: ● under dry argon; ○, under argon saturated with water vapor; ▲, under water; □, exposed to laboratory atmosphere. Note that rinsing with ether removed the hydrophobic contaminants adsorbed on the surface of the films.

Figure 6. ATR-IR spectra of samples of polyethylene: following extraction (PE-H); after oxidation (PE-COOH); after treatment with 1 N NaOH (PE-COO⁻); following treatment with NaBH₄, shown after equilibration of the surface at pH 3 and at pH 13; and following treatment with 1 M BH₃·THF (PE-CH₂OH).

Figure 7. ESCA (XPS) survey spectra of unoxidized and oxidized polyethylene (top left) and the composition of the surface of PE-CO₂H (top right) determined by integrating the peaks obtained by analyzing only over the binding energies characteristic of elements of interest (bottom).³⁷

Figure 8. Schematic representations of possible structures of PE-CO₂H. In each, A = CO₂H, =O = ketone, and \sim = -(CH₂)_n-. Each is drawn as if the polyethylene chains entering the oxidized region were crystalline; the argument is not changed if they are amorphous. Model A represents a limit of surface oxidation. The surface is rough, but no acid groups exist in the interior of the polymer. B represents a more plausible model: the groups in contact with water are a mixture of carboxylic acid, ketone, and methylene groups. Oxidized moieties also are found in the subsurface region. Although two acid groups do not exist on a single short polyethylene chain, a ketone can exist on a chain terminated by an acid group. Model C cannot represent the surface. The oxidation reaction does not introduce oxidized groups as branches, and low molecular weight species would be lost from the material on rinsing with water.

Figure 9. SEM micrographs of unoxidized and oxidized polyethylene; the micrograph labeled "60 sec oxidation" is of a sample representative of those used in this work; that labeled "6 min oxidation" is more heavily etched. The films are coated with ~200 Å of Au/Pd (5% Pd).

Figure 10. ATR-IR spectra of the carbonyl region of derivatives of PE-COOH.

Figure 11. Dependence of θ_a on pH (unbuffered solutions; pH adjusted with NaOH or HCl) for PE-COOH and several derivatives. The PE-CO₂CH₃ samples were made as follows: ○, by acid-catalyzed esterification; ●, by reaction with diazomethane; ◐ by reaction of PE-COCl and CH₃OH.

Figure 12. ATR-IR spectra of PE-COOH (left) and PE-CO₂H after treatment with NaBH₄ to remove ketone and aldehyde functionality (right) at several values of pH.

Figure 13. Extent of ionization α_i (eq 3) obtained for PE-CO₂H as a function of pH using ATR-IR spectroscopy. The experimental points are taken from the types of experiments summarized in Figure 12 using eq 8 and 9. The cross-hatched oval at pH 8 contains the data points determined using seven buffers (0.01 M).⁴⁵ Other curves shown are for acetic acid⁴³ and polyacrylic acid (PAA).⁴⁴

Figure 14. Variation in the measured value of θ as a function of the interval between application of the drop to the surface and the measurement. Data points are for typical single drops;

●, applied and measured under air saturated with water vapor (100% relative humidity); ○, applied at ambient humidity and then raised to 100% relative humidity; ◇, applied and kept at ambient humidity.

Figure 15. Dependence of θ_a on pH for PE-CO₂H with various pretreatments: ○, dry film; □, film equilibrated at pH 13 (NaOH) for 3 h, then washed in distilled water for 5 min, and dried in air for 30 min; ◇, film equilibrated at pH 1 (HCl) for 3 h, then washed and dried as above; ●, film subjected to five cycles between pH 1 and pH 13 (5 min each) then washed in distilled water for 5 min and dried. The results for UHMW-CO₂H (no pretreatment) are included (●).

Figure 16. Dependence of θ_a on pH for surface functionalized polyethylenes. Top: Using unbuffered aqueous solutions (pH adjusted with NaOH or HCl). Bottom: Using buffered aqueous solutions.⁴⁵ Buffers used: \square , 0.1 M phosphate buffer; \circ , all others (0.05 M) as follows: pH 1, 0.1 N HCl; pH 2, maleic acid; pH 3, tartaric acid; pH 4, succinic acid; pH 5, acetic acid; pH 6, maleic acid; pH 7 and pH 8, HEPES; pH 9 and pH 10, CHES; pH 11, triethylamine; pH 12, phosphate; pH 13, 0.1 N NaOH. The cross-hatched oval labeled "assorted buffers" at pH 8 includes data for phosphate, MOPS, HEPES, TAPS, TRIS, triethanolamine.

Figure 17. Dependence of θ_a on pH using different buffer concentrations on PE-CO₂H. Buffers used are the same as Figure 16 except at 1.0 M where liquid/vapor surface tension changes and ionic strength effects on θ_a can be significant. At 1.0 M the following buffers were substituted: pH 6 and pH 7, ethylenediamine; pH 8, Tris; pH 9 and pH 10, glycine; pH 11, γ -aminobutyric acid.

Figure 18. Extent of ionization, α_i , as a function of pH for PE-CO₂H: \bullet , using phosphate buffer; \blacklozenge , using organic buffers. The dashed line summarizes the ATR-IR data from Figure 13 for comparison. Data obtained by direct potentiometric titration of granular PE-CO₂H, \circ , are also shown.

Figure 19. Top: Dependence of pH of UHMW-CO₂H suspended in water (●) and of water alone (○) as a function of added 0.1 N NaOH.

Bottom: Ionization (α_i) of UHMW-CO₂H as a function of pH:

● , determined from the data in the upper part of this Figure using eq 10 for UHMW-CO₂H chips; ○ , determined from changes in θ_a with pH (Figure 15) for UHMW-CO₂H sheet.

Figure 20. Ionization (α_i) determined by direct potentiometric titration as a function of pH for: ● , granular PE-CO₂H; ○ , granular PE-CO₂H derived from hydrolyzed granular PE-CO₂OCH₃; ◆ , granular PE-CO₂H in the presence of 0.1 M NaCl.

Figure 21. Variation in the effective or apparent pK_a (pK_a^{eff} , eq 11) with the extent of ionization. The dashed line represents a visual fit of eq 10 to data of the sort in Figure 18 shown as ● . Curves for poly(acrylic acid) (PAA)⁴⁴ and CH₃CO₂H⁴³ are included for comparison.

Figure 22. Effects of added salts on θ_a and α_i as functions of pH (all systems were buffered with 0.05 M organic buffers). Salts used: ◆ , 1 M LiCl; ○ , no added salts; □ , 0.1 M CaCl₂.

Figure 23. Dependence of the $pK_a^{1/2}$ of PE-CO₂H on aqueous salt concentration: ◆ , NaNO₃; ○ , LiCl; □ , CaCl₂;

○ , NaCl. All solutions also contain 0.05 M buffer. Data for CH₃CO₂H⁴³ and polyacrylic acid (PAA)⁴⁴ in aqueous NaCl are also shown.

Figure 24. Effect of ionic strength (I) on $\cos \theta_a$ for PE-H and PE-CO₂H.

Salts used: ●, ○, NaClO₄; ▲, △, (NH₄)₂SO₄; ■, NaI; ◆, ◇, AlCl₃. The changes in $\cos \theta_a$ predicted from changes in γ_{LV} alone (eq 12), using values of γ_{LV} for (NH₄)₂SO₄ as representative are shown for comparison.

Figure 25. Schematic diagrams illustrating three possible factors influencing the ionization of surface-bound carboxylic acids. These are: A, ion-ion interactions; B, dipolar interactions between the functional groups on the surface and the solvent; C, the low "average" dielectric constant of the PE-CO₂H/H₂O interface.

Scheme I. Reactions used to convert the carboxylic acid groups of PE-CO₂H to derivatives.

Acid-Base Behavior of Carboxylic Acid Groups Covalently Attached at the
Surface of Polyethylene: The Usefulness of Contact Angle in Following the
Ionization of Surface Functionality

Stephen Randall Holmes-Farley, Robert H. Reamey, Thomas J. McCarthy, John
Deutch, and George M. Whitesides*

Supplementary Material for Microfilm Edition

The Surface Area under a Drop As a Function of Contact Angle

From the geometry of Figure 1 we have the following relations:

$$x^2 + p^2 = r^2 \quad r = \frac{d}{2 \sin \theta} \quad y = r \cos \theta$$

By integrating circular slabs of volume along p we get

$$\text{Volume in drop} = V = \int_y^r \pi x^2 dp$$

$$V = \int_y^r \pi (r^2 - p^2) dp = \pi \left[\int_y^r r^2 dp - \int_y^r p^2 dp \right]$$

$$V = \pi \left[r^2 p \Big|_y^r - \frac{1}{3} p^3 \Big|_y^r \right]$$

$$V = \pi r^2 [r - y] - \frac{1}{3} r^3 + \frac{1}{3} y^3 = \pi r^3 \left[\frac{2}{3} - \cos \theta + \frac{\cos^3 \theta}{3} \right]$$

$$V = \frac{\pi d^3}{8 \sin^3 \theta} \left[\frac{2}{3} - \cos \theta + \frac{\cos^3 \theta}{3} \right]$$

Solving for d^3 we get

$$d^3 = \frac{8V \sin^3 \theta}{\pi} \left[\frac{2}{3} - \cos \theta + \frac{\cos^3 \theta}{3} \right]$$

The surface area under the drop = $S = \pi \left(\frac{d}{2} \right)^2 = \frac{\pi}{4} d^2$

$$S = \pi \left[\frac{V^{2/3} \sin^2 \theta}{\pi^{2/3}} \right] \left[\frac{2}{3} - \cos \theta + \frac{\cos^3 \theta}{3} \right]^{-2/3}$$

$$S = \pi^{1/3} V^{2/3} \sin^2 \theta \left[\frac{2}{3} - \cos \theta + \frac{\cos^3 \theta}{3} \right]^{-2/3}$$

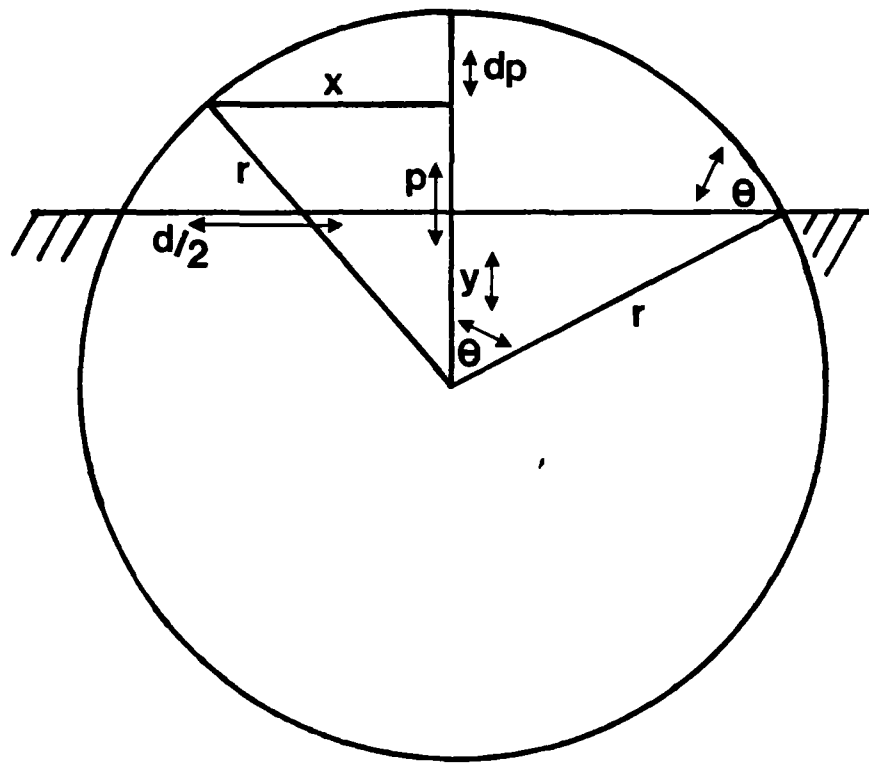


Figure 1

APPENDIX

DL/413/83/01
GEN/413-2

TECHNICAL REPORT DISTRIBUTION LIST, GEN

	<u>No. Copies</u>		<u>No. Copies</u>
Office of Naval Research Attn: Code 413 800 N. Quincy Street Arlington, Virginia 22217	2	Naval Ocean Systems Center Attn: Technical Library San Diego, California 92152	1
ONR Pasadena Detachment Attn: Dr. R. J. Marcus 1030 East Green Street Pasadena, California 91106	1	Naval Weapons Center Attn: Dr. A. B. Amster Chemistry Division China Lake, California 93555	1
Commander, Naval Air Systems Command Attn: Code 310C (H. Rosenwasser) Washington, D.C. 20360	1	Scientific Advisor Commandant of the Marine Corps Code RD-1 Washington, D.C. 20380	1
Naval Civil Engineering Laboratory Attn: Dr. R. W. Drisko Port Hueneme, California 93401	1	Dean William Tolles Naval Postgraduate School Monterey, California 93940	1
Superintendent Chemistry Division, Code 6100 Naval Research Laboratory Washington, D.C. 20375	1	U.S. Army Research Office Attn: CRD-AA-IP P.O. Box 12211 Research Triangle Park, NC 27709	1
Defense Technical Information Center Building 5, Cameron Station Alexandria, Virginia 22314	12	Mr. Vincent Schaper DTNSRDC Code 2830 Annapolis, Maryland 21402	1
DTNSRDC Attn: Dr. G. Bosmajian Applied Chemistry Division Annapolis, Maryland 21401	1	Mr. John Boyle Materials Branch Naval Ship Engineering Center Philadelphia, Pennsylvania 19112	1
Naval Ocean Systems Center Attn: Dr. S. Yamamoto Marine Sciences Division San Diego, California 91232	1	Mr. A. M. Anzalone Administrative Librarian PLASTE/ARRADCOM Bldg 3401 Dover, New Jersey 07801	1

ABSTRACTS DISTRIBUTION LIST, 356B

Professor A. G. MacDiarmid
Department of Chemistry
University of Pennsylvania
Philadelphia, Pennsylvania 19174

Dr. E. Fischer, Code 2853
Naval Ship Research and
Development Center
Annapolis, Maryland 21402

Professor H. Allcock
Department of Chemistry
Pennsylvania State University
University Park, Pennsylvania 16802

Professor R. Lenz
Department of Chemistry
University of Massachusetts
Amherst, Massachusetts 01002

Professor M. David Curtis
Department of Chemistry
University of Michigan
Ann Arbor, Michigan 48105

Dr. J. Griffith
Naval Research Laboratory
Chemistry Section, Code 6120
Washington, D.C. 20375

Professor G. Wnek
Department of Materials Science
and Engineering
Massachusetts Institute of Technology
Cambridge, Massachusetts 02139

Mr. Samson Jennekke
Honeywell Corporate Technology Center
10701 Lyndale Avenue South
Bloomington, Minnesota 55420

Dr. Richard M. Laine
SRI International
333 Ravenswood Avenue
Menlo Park, California 94025

Dr. James McGrath
Department of Chemistry
Virginia Polytechnic Institute
Blacksburg, Virginia 24061

Dr. Adolf Amster
Chemistry Division
Naval Weapons Center
China Lake, California 93555

Professor C. Allen
Department of Chemistry
University of Vermont
Burlington, Vermont 05401

Dr. William Tolles
Code 6100
Naval Research Laboratory
Washington, D.C. 20375

Professor T. Katz
Department of Chemistry
Columbia University
New York, New York 10027

Professor J. Salamone
Department of Chemistry
University of Lowell
Lowell, Massachusetts 01854

Professor J. Chien
Department of Chemistry
University of Massachusetts
Amherst, Massachusetts 01854

Professor William R. Krigbaum
Department of Chemistry
Duke University
Durham, North Carolina 27706

Dr. R. Miller
IBM Research Laboratory K42/282
5600 Cottle Road
San Jose, California 95193

DL/413/83/01
356B/413-2

ABSTRACTS DISTRIBUTION LIST, 356B

Professor T. Marks
Department of Chemistry
Northwestern University
Evanston, Illinois 60201

Professor Malcolm B. Polk
Department of Chemistry
Atlanta University
Atlanta, Georgia 30314

Dr. Kurt Baum
Fluorochem, Inc.
680 S. Ayon Avenue
Azusa, California 91702

Professor H. Ishida
Department of Macromolecular Science
Case Western University
Cleveland, Ohio 44106

Professor Stephen Wellinghoff
Department of Chemical Engineering
University of Minnesota
Minneapolis, Minnesota 55455

Professor G. Whitesides
Department of Chemistry
Harvard University
Cambridge, Massachusetts 02138

Dr. K. Paciorek
Ultrasystems, Inc.
P.O. Box 19605
Irvine, California 92715

Professor H. Hall
Department of Chemistry
University of Arizona
Tucson, Arizona 85721

Professor D. Seyferth
Department of Chemistry
Massachusetts Institute of Technology
Cambridge, Massachusetts 02139

TECHNICAL REPORT DISTRIBUTION LIST, GEN

	<u>No.</u> <u>Copies</u>		<u>No.</u> <u>Copies</u>
Office of Naval Research Attn: Code 413 800 N. Quincy Street Arlington, Virginia 22217	2	Naval Ocean Systems Center Attn: Technical Library San Diego, California 92152	1
ONR Pasadena Detachment Attn: Dr. R.J. Marcus 1030 East Green Street Pasadena, California 91106	1	Naval Weapons Center Attn: Dr. A.B. Amster Chemistry Division China Lake, California 93555	1
Commander, Naval Air Systems Command Attn: Code 310C (H. Rosenwasser) Washington, D.C. 20360	1	Scientific Advisor Commandant of the Marine Corps Code RD-1 Washington, D.C. 20380	1
Naval Civil Engineering Laboratory Attn: Dr. R.W. Drisko Port Hueneme, California 93401	1	Dean William Tolles Naval Postgraduate School Monterey, California 93940	1
Superintendent Chemistry Division, Code 6100 Naval Research Laboratory Washington, D.C. 20375	1	U.S. Army Research Office Attn: CRD-AA-IP P.O. Box 12211 Research Triangle Park, NC 27709	1
Defense Technical Information Center Building 5, Cameron Station Alexandria, Virginia 22314	12	Mr. Vincent Schaper DTNSRDC Code 2830 Annapolis, Maryland 21402	1
DTNSRDC Attn: Dr. G. Bosmajian Applied Chemistry Division Annapolis, Maryland 21401	1	Mr. John Boyle Materials Branch Naval Ship Engineering Center Philadelphia, Pennsylvania 19112	1
Naval Ocean Systems Center Attn: Dr. S. Yamamoto Marine Science Division San Diego, California 91232	1	Mr. A.M. Anzalone Administrative Librarian PLASTEC/ARRADCOM Bldg. 3401 Dover, New Jersey 07801	1

ABSTRACTS DISTRIBUTION LIST, 3568

Professor A. G. MacDiarmid
Department of Chemistry
University of Pennsylvania
Philadelphia, Pennsylvania 19174

Dr. E. Fischer, Code 2853
Naval Ship Research and
Development Center
Annapolis, Maryland 21402

Professor H. Allcock
Department of Chemistry
Pennsylvania State University
University Park, Pennsylvania 16802

Professor R. Lenz
Department of Chemistry
University of Massachusetts
Amherst, Massachusetts 01002

Professor M. David Curtis
Department of Chemistry
University of Michigan
Ann Arbor, Michigan 48105

Dr. J. Griffith
Naval Research Laboratory
Chemistry Section, Code 6120
Washington, D.C. 20375

Professor G. Wnek
Department of Materials Science
and Engineering
Massachusetts Institute of Technology
Cambridge, Massachusetts 02139

Mr. Samson Jennekke
Honeywell Corporate Technology Center
10701 Lyndale Avenue South
Bloomington, Minnesota 55420

Dr. Richard M. Laine
SRI International
333 Ravenswood Avenue
Menlo Park, California 94025

Dr. James McGrath
Department of Chemistry
Virginia Polytechnic Institute
Blacksburg, Virginia 24061

Dr. Adolf Amster
Chemistry Division
Naval Weapons Center
China Lake, California 93555

Professor C. Allen
Department of Chemistry
University of Vermont
Burlington, Vermont 05401

Dr. William Tolles
Code 6100
Naval Research Laboratory
Washington, D.C. 20375

Professor T. Katz
Department of Chemistry
Columbia University
New York, New York 10027

Professor J. Salamone
Department of Chemistry
University of Lowell
Lowell, Massachusetts 01854

Professor J. Chien
Department of Chemistry
University of Massachusetts
Amherst, Massachusetts 01854

Professor William R. Krigbaum
Department of Chemistry
Duke University
Durham, North Carolina 27706

Dr. R. Miller
IBM Research Laboratory K42/282
5600 Cottle Road
San Jose, California 95193

ABSTRACTS DISTRIBUTION LIST, 356B

Professor T. Marks
Department of Chemistry
Northwestern University
Evanston, Illinois 60201

Professor Malcolm B. Polk
Department of Chemistry
Atlanta University
Atlanta, Georgia 30314

Dr. Kurt Baum
Fluorochem, Inc.
680 S. Ayon Avenue
Azusa, California 91702

Professor H. Ishida
Department of Macromolecular Science
Case Western University
Cleveland, Ohio 44106

Professor Stephen Wellinghoff
Department of Chemical Engineering
University of Minnesota
Minneapolis, Minnesota 55455

Professor G. Whitesides
Department of Chemistry
Harvard University
Cambridge, Massachusetts 02138

Dr. K. Paciorek
Ultrasystems, Inc.
P.O. Box 19605
Irvine, California 92715

Professor H. Hall
Department of Chemistry
University of Arizona
Tucson, Arizona 85721